

1 **RESPONSE TO THE REVIEWS**

2 We would like to thank both Reviewers for their careful and constructive reviews of our  
3 paper. In response to their suggestions, we did the following main changes to the  
4 manuscript:

- 5 - we revised the manuscript focusing on the main objective that is the application of the  
6 SfM-MVS method for monitoring glacial and periglacial processes. Therefore we changed  
7 the title, we modified the abstract accordingly, providing quantitative information about the  
8 obtained results and we reduced the introduction.
- 9 - we modified the structure as suggested by the Reviewer 2, moving the paragraphs about  
10 the formula of photogrammetric depth accuracy and the mass balance calculation method  
11 in section 3.3.
- 12 - we made the figures and legends uniform using two decimal places and we changed the  
13 intervals of the maps of the elevation difference.
- 14 - as suggested by the Reviewer 1 we analyzed the relationship between the viewshed  
15 analysis and the elevation accuracy considering all camera positions. Furthermore we  
16 included in the plot the mean of the absolute values of the Z differences.
- 17 - we implemented the suggested changes and answered to the specific comments made by  
18 the reviewers, as detailed in the following of this document.

19

20 **REVIEWER 1**

21 **General Comments:**

NOTES	CORRECTIONS
<p>This paper presents an application of the automatic photogrammetry technique known as Structure-from-Motion to investigate glacial and periglacial processes in the Italian Alps. Authors assess the accuracy of datasets acquired during field surveys using ALS datasets as benchmark. These techniques are of growing interest for Geoscientists and, in my opinion, the paper deserves for the definitive publication in Earth Surface Dynamics. The structure is correct, the methods are properly executed and described and results are, in my opinion, interesting for the scientific community. I include below some minor suggestions or comments that could be of interest for the authors to be incorporated in the final version of the manuscript.</p>	<p>The manuscript has been edited following the reviewer's comments and suggestions.</p>

22

23 **Specific Comments:**

NOTES	CORRECTIONS
<p>1) THE TITLE: In my opinion, the title does not describe exactly the content of the paper</p>	<p>We agree with the reviewer on the relative importance of the contributions. According to the</p>

because currently the title “Analysis of glacial and periglacial processes using SfM” focus on the processes. The processes are addressed in the paper, but the focus is set on the factors influencing the accuracy of the SfM models. The time devoted to understand the global and spatial distribution of the accuracies is longer than the time used to explain the glacial and periglacial processes. I suggest that this aspect should be included in a new title for the paper. Something like “Analyzing the suitability-accuracy of SfM to monitor glacial and periglacial processes...” would be more adequate in my opinion.

suggestion, we changed the title in: “Suitability of ground-based SfM-MVS for monitoring glacial and periglacial processes”

2) REAL LEVEL OF GEOMORPHIC CHANGE AND LEGEND INTERVALS: In some figures (for example figure 6 or 19) present a different number of decimal places in the legend, I recommend you to be consistent and the use of the same number of decimal places for the intervals.

We made the figures and legends uniform using two decimal places, as suggested.

On the other hand, the use of intervals or classes smaller than 1 m in the legend, in my opinion, is not supported by your results. I mean, if you are getting accuracies of around 1 m, using intervals from -0.05 to 0.05 (i.e. 10 cm) is below your real level of detection. I recommend fitting the legend of these figures to the real accuracy of you datasets.

Regarding the choice of the interval of the elevation differences between the SfM-MVS DEMs and the ALS DEM, we tried to find a good compromise between the obtained accuracy and the need for an efficient visualization of the analyzed glacial and periglacial processes. Therefore, we decided to distinguish the positive and negative values using intervals lower than 1 m for both case studies. Different intervals for the two surveyed areas were chosen according to the different resolution and accuracy of the SfM-MVS DEMs. For the glacier we extended the interval around zero to +/- 0.25 m; for the rock glacier we changed the interval to +/- 0.10 m. While the overall accuracy is limited, as correctly noted, rather in the meter (or a bit better) domain, there are still large areas, where conditions are better, and the accuracy is higher. Thus, also large areas with differences below +/- 10cm are given. With the legend we do not want to claim, that we can detect 10cm differences everywhere.

3) 3D SURFACE CHANGES: The estimated changes among the different DTMs are assumed to happen in a predominant way in the vertical direction, i.e. the vector of change is normal to the horizontal plane, which is not very often the case in mountainous and glacier landscapes. It is well known that DTMs are not real 3D records of the landscape. In my opinion, the use of an

In this paper we analyzed i) elevation changes and ii) surface displacement rates. The first is computed along the vertical direction, by definition. The second is calculated in the horizontal plane, and are not the result of DoD. 3D displacements in rock glaciers are the result of vertical and horizontal components, but in our case only horizontal components were of interest. Sentence

analysis based on 2.5D datasets (DTMs) and reference added in Section 3.3. instead of 3D actual approaches should be justified and discussed on the manuscript. In your case it is quite a simple issue because the most interesting area for you is the glacier that presents low slopes and changes tend to happened in the vertical direction (which is the one that you assume when you use a DoD approach).

4) LINE OF SIGHT ANALYSIS: The analysis of the relationship between the line of sight and the elevation difference is limited to the line of sight for a specific camera (five camera locations); however, I guess that from a methodological viewpoint it would be logical to investigate the average incidence angle for a cell (estimating the average angle using every camera) and the Z difference. Additionally, the number of times every pixel is visible from a camera can explain a part of the variance in Z differences. This analysis would be interesting, otherwise you could justify that the selected camera is representative of a number of camera poses.

As suggested, we calculated the mean of the incidence angle considering 5 representative camera positions.

We analyzed the relationship between the viewshed analysis and the elevation accuracy considering all camera positions.

5) DTM, DEM and DSM: Along the paper, the DTM term is used to describe the gridded model resulting from the processing of the point clouds. The term DTM is widely used to describe models representing different topographic attributes (i.e. elevation, slope gradient, curvature, etc.). In this line, the term DEM is specifically used to describe the DTM that represents the altitude and the term DSM is specifically used to describe the Digital Surface Model. I recommend to use the specific acronyms in the text to avoid misunderstandings.

We used the suggested terminology changing the acronyms from DTM to DEM.

24

25 **Technical corrections:**

NOTES	CORRECTIONS
L5-P4, L10-P4, I suggest the use of uppercases for "lidar", please extend this to rest of the manuscript.	Ok, modified accordingly with LiDAR

L9-P4, I suggest the use of consumer-grade or conventional instead “common”.	Ok, edited.
L22-L26-P4, In general and along the manuscript, I suggest the use of the passive voice instead of the first person style. For example, L6-P13 (1357) “the accuracy of the photogrammetric reconstruction for the different substrata was investigated” instead of “WE : : :”.	Ok, modified accordingly.
L23- P5, I suggest the use of “repeated” instead of “repeat”	Ok, edited.
L17-P7, You refer to Figure 4, however, in the list of figures, this figure presents the workflow instead the location of the camera, and I guess you refer to figure 5, please check.	Ok, modified accordingly.
L29- P11, I suggest leaving out the last sentence about the unfavorable line of sight because later, you will state that there is not significant relationship between the incidence angle (line of sight to normal vector) and Z differences.	Actually we found a significant correlation between the mean of the incidence angles and the elevation differences, so we kept this sentence.
L29- P11, I suggest trying to explain this 0.41 m mean value for 0-10 degrees of slope areas using the visual and physical properties of the materials. Probably differences in texture or any other aspect are causing this value to be higher than expected.	The role of the surface texture and unfavorable line of sight is already mentioned in the text. We edited the text to improve clarity.
L15- P17, longer than what? I suggest the use of “long”.	Ok, edited accordingly.
TABLE 5: please check caption: “: : : stable are off: : :” .	Ok, fixed.
FIGURE 1: I recommend a thicker line to delineate the glaciers.	In our opinion the line is thick enough, but we will consider thickening it when we have the final layout of the figure.
FIGURE 5: I understand that you are using the same north arrow and scale bar for the a) and b) maps and I recommend you to include these between the two maps and not inside b).	Ok, modified accordingly.
FIGURE 6: please use the same number of significant decimal places in the legend. On the other hand, and according to your methods.	Ok, we changed the decimal using two decimal places. Regarding the choice of intervals, please see the comments above in "Specific comments

I think is not justified the use of intervals in the legend smaller than 1 m, you are using a DTM of 1 m pixel size and your estimations of the vertical accuracy of the SFM-DTMs clearly point out to a level of detection of geomorphic change > 1 m. (2)".

FIGURE 7: For me it is very difficult to understand figure 7 in its present form. The lines of the profile are superimposed and even in the zoom window, it is difficult. I do not understand how you include camera locations in a 2 dimensional plot.

We fully agree that the lines of the profiles are superimposed, because there is no exaggeration of the elevation values but we maintained the same scale for both axis. However, the plot on the bottom show the differences between the elevation profiles with large scale (+-3m). Both profiles and the camera positions were projected onto the xz-plan. We removed the inset and we added an explanation in the figure caption.

FIGURE 8: the legend of figure 8b could be located on the bottom-right part of the graph for a better visibility of the columns.

As suggested we included in the plot the mean of the absolute values of the Z differences. We improved the location of the legends in the figure. Errors for high-slope areas in bare ground are likely due to residual inaccuracies deriving from the use of natural features as GCPs. Sentence added in the text.

The mean and the standard deviation are good parameters but I miss in your manuscript the use of an absolute value of the differences that probably would correlate with slope. The mean value is not very rich unless you have systematics errors in your data. This is the case of high slopes in bare ground, any explanation?

FIGURE 9: an interesting approach here would be the analysis of the relationship between the number of times an object is visible from a different camera and the Z differences.

We changed the figure according to the suggested analyses. The results were added in the text (Section 4.1)

FIGURE 19: please use the same number of significant decimal places in the legend. On the other hand, and according to your methods I think is not justified the use of intervals in the legend smaller than 1 m, you are using a DTM of 1 m pixel size and your estimations of the vertical accuracy of the SFM-DTMs clearly point out to a level of detection of geomorphic change > 1 m.

Ok, we changed the decimal using two decimal places for each interval. See the reply to the Specific Comment (2) for the choice of intervals.

26  
27  
28  
29

30 **REVIEWER 2 – C508**

31 **General Comments:**

NOTES	CORRECTIONS
<p>The manuscript by Piermattei et al. compares the outcome the use of terrestrial photogrammetry using normal digital images and subsequent Structure from motion (SfM) analysis with laser scans as a benchmark. For geomorphologists working with surface changes and movements SfM combined with careful measurements of GCPs is a highly valuable tool to address surface dynamics easily and with a high accuracy. The manuscript does not give scientifically completely new information or techniques, but reproduces findings by other colleagues, and comes up with useful recommendations. These are certainly helpful for other colleagues, especially when working in high-alpine or arctic environments. Within this respect the manuscript is a valuable contribution for the geomorph community and deserved attention. The manuscript has some issues which should be addressed before publications. I here only focus on general issues, smaller details are already addressed by the other reviewer and needs not to be duplicated.</p>	<p>The manuscript has been edited following the reviewer's comments and suggestions.</p>

32

33 **Specific Comments:**

NOTES	CORRECTIONS
<p>1. Title: As review 1, change the title, I strongly support this</p>	<p>The title was change in: "Suitability of ground-based SfM-MVS for monitoring glacial and periglacial processes"</p>
<p>2. Abstract: The abstract is lengthy and very general, you should give some major results and key numbers there (e.g. some obtained accuracies and major finding etc).</p>	<p>We modified the abstract accordingly, providing quantitative information about the obtained results for both case studies.</p>
<p>3. Focus: The focus is on the techniques, not necessarily on the interpretation of glacial/periglacial processes. It is enough to write that the measured changes are in line with field-based mass balance measurements, or the velocities obtained on</p>	<p>According to the suggestion of the Reviewer we moved this paragraph in section 3.3 and significantly reduced it</p>

the rock glacier seems ok.

P. 1359, the whole paragraph is a method, and should be moved there, but I would simply suggest strongly reducing this part (along with changing the title). If you want to keep it as is, you should also really discuss the geomorphology/glaciology, but this would change focus of the paper.

4. Introduction: Lengthy, lots of citations, and is almost a small review. Maybe there should be a review about SfM applications and limitations in geomorphology, but this is not the focus of your paper. So I would reduce the intro, and really focus on what you want to tell the reader. Your main message is that SfM is “easy” and especially “cost-effective” monitoring for many researchers, even in difficult places. I agree, so emphasize on that, and emphasize to come up with clear recommendations, other colleagues can find useful.

We reduced the introduction as suggested, focusing on the SfM technique and emphasizing the advantages of this survey technique.

5. Case study: p. 1349, maybe “Setting” is better as heading

We modified the heading as follows: “Geographical setting and case studies”

6. Method: p 1350, l 5: This introduction is not necessary, takes only space.

Ok, we removed this paragraph.

7. Results: There are several places, you introduce new methods in the result chapter, and this is a bit confusing, like on p. 1356 and 1359. Consider to revise.

We moved the methodological parts in Section 3.3, as suggested.

For the maps of elevations changes, also consider to enlarge a bit the areas without significant changes, or give a reason of choice or the classification in the figure (Fig. 6 etc). As you of course are aware of, considering general error propagation laws, the mean error adds up, and this gives large relative errors when subtract things. Like Fig. 14, the colorless class is +- 5 cm, is this justified or should then class be bigger?

We slightly modified the figures, increasing the interval in grey color, i.e. with no significant changes. Please, see the reply to the Specific Comment (2) by Reviewer 1.

And: Be careful with the term “geodetic mass balance” for a one year period, as ice fluxes and varying snow density or re-freezing of melt water is not taken into account. The

In the paper we estimated the geodetic mass balance from surface elevation changes, without considering other processes. In our opinion, given the specific case study, this is a reasonable

latter is certainly important on small glaciers in a permafrost environments, however, small glaciers have normally little ice fluxes, probably compensating other factors. simplification. Clarified in the text (Section 3.3).

8. Discussion: Could be structured with two headings: Maybe: "Data processing and assessment" and "Recommendations" or so. We divided the Discussion according to the suggestion of the Reviewer.

9. Figures: These are certainly nice, but unfortunately totally unreadable because of small size. I had to use the original pdf and zoom 589% to read the smallest numbers :-)  
The only figure which is readable is Fig. 14. Therefore it is also the only one I have commented above. Only printing this is totally useless. We agree some figure are small, in particular the legend. However, we will check appropriate figure sizes when we have the layout.

Maybe the numbers of Figures (#20!) is a bit too much, so check if some of the figures you want to give can be coupled somehow, or if all are really necessary. We preferred to keep all figures because we consider them important for a better understanding of the results.

34  
35



# Suitability of ground-based SfM-MVS for monitoring glacial and periglacial processes

## Analysis of glacial and periglacial processes using structure from motion

L. Piermattei<sup>1</sup>, L. Carturan<sup>1</sup>, F. de Blasi<sup>1</sup>, P. Tarolli<sup>1</sup>, G. Dalla Fontana<sup>1</sup>, A. Vettore<sup>2</sup> and N. Pfeifer<sup>3</sup>.

<sup>1</sup>Department of Land, Environment, Agriculture and Forestry, University of Padova, Italy

<sup>2</sup>Interdepartment Research Center of Geomatics, University of Padova, Italy

<sup>3</sup>Department of Geodesy and Geoinformation, TU Wien, Austria

Correspondence to: L. Piermattei (livia.piermattei@studenti.unipd.it)

### **Abstract**

~~PClose-range~~ photo-based surface reconstruction from the ground is rapidly emerging as an alternative survey technique to LiDAR (light detection and ranging), ~~which today represents the main survey technique~~ in many fields of geoscience, ~~fostered by the recent~~. ~~The recent evolution of photogrammetry, incorporating development of~~ computer vision algorithms such as Structure from Motion (SfM) and dense image matching such as Multi-View Stereo (MVS), ~~allows the reconstruction of dense 3-D point clouds for the photographed object from a sequence of overlapping images taken with a digital consumer camera.~~ The objective of ~~our~~ this work was to test the accuracy of suitability of the ground-based SfM-MVS approach in calculating the geodetic mass balance of a 2.1 km<sup>2</sup> glacier and for the detection of the surface displacement rate of a neighbouring active rock glacier located in the Ortles-Cevedale Group, in the Eastern Italian Alps. ~~In addition, we investigated the feasibility of using the image-based approach for the detection of the surface displacement rate of a neighbouring active rock glacier. The terrestrial surveys were photos were acquired in 2013 and 2014 using a digital consumer-grade camera, organizing single-day field surveys, planned to be quick with a low budget and conducted in a safe and easy way in a single day.~~ Airborne laser scanning (ALS) data were used as benchmarks to estimate the accuracy of the photogrammetric digital elevation models (DEMs) and the reliability of the method, ~~in this specific applications.~~ The ~~results were encouraging because the~~ SfM-MVS approach enabled sd the reconstruction of high-quality DEMs, which provided estimates of glacial

69 and periglacial processes similar to those achievable by ALS. ~~The glacial and~~  
70 ~~periglacial analyses were performed using both range and image-based surveying~~  
71 ~~techniques, and the results were then compared.~~ In stable bedrock areas outside the  
72 glacier, the accuracy of the photogrammetric DEMs, evaluated as the mean and  
73 the standard deviation of the elevation difference in a stable area between the SfM-  
74 MVS DEM and the reference ALS DEM, was  $-0.42\text{ m} \pm 1.72\text{ m}$  and  $0.03\text{ m} \pm 0.74\text{ m}$   
75 for their 2013 and 2014 surveys, respectively. In the rock glacier area, the elevation  
76 difference was ~~The SfM-MVS DEM accuracy of the reconstructed rock glacier surface~~  
77 acquired in 2014 was estimated to be  $0.02\text{ m} \pm 0.17\text{ m}$ . The use of natural targets as  
78 ground control points, the occurrence of shadowed and low-contrast areas, and in  
79 particular the sub-optimal camera network geometry imposed by the morphology of  
80 the study area were the main factors affecting the accuracy of photogrammetric  
81 DEMs.

82 ~~Different resolutions and accuracies were obtained for the glacier and the rock~~  
83 ~~glacier, given the different survey geometries, surface characteristics and areal~~  
84 ~~extents. The analysis of the SfM-MVS DEM quality allowed us to highlight the~~  
85 ~~limitations of the adopted expeditious method in the studied alpine terrain and the~~  
86 ~~potential of this method in the multitemporal study of glacial and periglacial areas.~~

87

## 88 **1. Introduction**

89 Knowledge of changes in the extent, mass and surface velocity of glaciers and rock  
90 glaciers contributes to better understanding the dynamic processes occurring in cold  
91 high-mountain environments and serves as an important contribution to climate  
92 monitoring (Kääb et al., 2003).

93 Numerous techniques exist for monitoring and quantifying these changes and include  
94 both field and remote sensing methods (Immerzeel et al., 2014). Fieldwork generally  
95 yields high-quality data but with a small spatial extent, given the remoteness and low  
96 accessibility of mountain areas at high elevations (Roer et al., 2007). Therefore,  
97 using remotely sensed datasets for at least two different points in time has become  
98 an important tool for monitoring high-mountain terrain dynamics (Kääb, 2002).

99 Multitemporal Digital Terrain Elevation Models (DEMs) based on remote sensing data  
100 are the most commonly used products for such investigations (Kääb, 2005; Tseng et  
101 al., 2015).

102 ~~Among the many remote sensing techniques, aerial photogrammetry is the oldest~~  
103 ~~method, and it has a long history of application in the study of glaciers (Welch and~~  
104 ~~Howarth, 1968; Käab and Funk, 1999; Schenk, 1999; Baltsavias et al., 2001; Käab~~  
105 ~~2005; Haug et al., 2009; Bühler et al., 2014; Müller et al., 2014) and the monitoring of~~  
106 ~~rock glaciers via repeated stereo images (Käab et al., 1997; Kaufmann, 1998; Käab,~~  
107 ~~2003; Fischer, 2011). Terrestrial (ground-based or close-range) photogrammetry was~~  
108 ~~one of the first measurement techniques used to map high mountain terrain and for~~  
109 ~~reliably measuring the flow velocity of a rock glacier (Kaufmann and Ladstädter 2007;~~  
110 ~~Kaufmann, 2012) until it was replaced by aerial and spaceborne platforms (Pellikka~~  
111 ~~and Rees, 2009).~~

112 ~~Over the last decade, the photogrammetric technique has widely been replaced by~~  
113 ~~LiDAR (light detection and ranging) technology, which has progressively become the~~  
114 ~~primary survey technique in geomorphology (Tarolli, 2014). Aerial laser scanning~~  
115 ~~(ALS) is reported to be a very accurate method for DEMs generation in alpine terrain~~  
116 ~~(Bühler and Graf, 2013; Aguilar and Mills, 2008; Höfle and Rutzinger, 2011), snow~~  
117 ~~covered areas (Höfle et al., 2007; Deems et al., 2013) and glacial environments~~  
118 ~~(Geist Stotter, 2007; Kodde et al., 2007; Abermann et al., 2010; Knoll and Kerschner,~~  
119 ~~2010; Carturan et al., 2013; Colucci et al., 2014; Joerg and Zemp, 2014). However,~~  
120 ~~aerial LiDAR surveys are still expensive and terrestrial LiDAR surveys involve~~  
121 ~~expensive and logistically demanding equipment.~~

122 Among the available remote sensing techniques, the~~The~~ close-range  
123 photogrammetry saw a rapid development thanks to the recent evolution of digital  
124 photogrammetry, based on computer vision algorithms. This technique is,~~has led to~~  
125 a rapid revival of close-range photogrammetry becoming as the major alternative to  
126 traditional surveying techniques and LiDAR (light detection and ranging)  
127 technologyies, due to its lower cost, high portability, and easy and rapid surveying in  
128 the field.

129 The photogrammetric approach known as Structure from Motion (SfM) allows to  
130 obtainsobtaining 3D information ~~on of~~ the photographed object from a sequence of  
131 overlapping images taken with a ~~consumer-grade~~ digital camera. ~~The ability to obtain~~  
132 ~~3D models with accuracies and resolutions comparable to those of LiDAR has~~  
133 ~~created new opportunities, especially in geoscience applications in remote areas~~  
134 ~~(James and Robson, 2012; Bemis et al., 2014; Micheletti et al., 2014; Prosdocimi et~~

135 ~~al., 2015; Stumpf et al., 2015). An overview of the SfM applications and accuracy~~  
136 ~~assessments is given by Clapuyt et al. (2015).~~

137 A limited number of ~~studies~~ applications of ~~close-range SfM~~ -photogrammetry in  
138 glacial and periglacial environments exists, and they principally involve the use of  
139 Unmanned Aerial Vehicles (UAVs) for image acquisition (Solbø S. and Storvold R.  
140 2013; Whitehead et al., 2013; Immerzeel et al., 2014, Tonkin et al., 2014; Gauthier et  
141 al., 2014; Bühler et al., 2014; Dall'Asta et al., 2015a; Ryan et al., 2015) rather than  
142 ground-based surveys (Gómez-Gutiérrez et al., 2014; 2015; Kääb et al., 2014;  
143 Piermattei et al., 2015). ~~Kääb et al. (2014) tested the time-lapse SfM approach in the~~  
144 ~~measurement of vertical and horizontal changes in periglacial patterned grounds.~~

145 The objective of our work was to assess the ~~potential and the limits~~ suitability of the  
146 ground-based SfM approach ~~in~~ for monitoring glacial and periglacial processes in a  
147 high-altitude area of the Ortles-Cevedale Group (Eastern Italian Alps). In particular,  
148 ~~we used the~~ this approach was used to calculate the geodetic annual mass balance  
149 of a 2.1 -km<sup>2</sup> glacier and to detect the surface displacement of a neighbouring 0.06 -  
150 km<sup>2</sup> rock glacier. The photogrammetric surveys were intentionally planned to be as  
151 quick and cost-effective as possible, and easily replicable in the future. Therefore, a  
152 consumer-grade camera was adopted to find an appropriate balance between the  
153 affordability and accessibility of the system (i.e. cost and ease of use) and the quality  
154 of the resulting topographic data (accuracy and density). The accuracy of the  
155 photogrammetric DEMs was estimated using ALS-based DEMs acquired during the  
156 same periods. The main factors affecting the accuracy of the photogrammetric DEMs  
157 were investigated, and the significance of the biases in the quantification of glacial  
158 and periglacial processes was discussed.

## 161 2. Geographical setting and ~~C~~ case studies

162 The La Mare Glacier and the neighbouring AVDM3 Rock Glacier are located in the  
163 south-eastern part of the Ortles-Cevedale massif (Eastern Italian Alps), the largest  
164 glaciated mountain group of the Italian Alps (Fig. 1).

165 The La Mare Glacier (World Glacier Inventory code I4L00102517; WGMS 1989) is a  
166 3.55 km<sup>2</sup> valley glacier currently composed of two ice bodies, which have different  
167 morphologies and tend to separate (Carturan et al., 2014). In this work, we focused

168 the focus was on the southern ice body, which feeds the main tongue. This 2.1 km<sup>2</sup>  
169 ice body primarily faces north-east, and its surface is rather flat, with the exception of  
170 the small remnant of its valley tongue. The elevation ranges from 2660 to 3590 m  
171 a.s.l. Mass balance investigations using the direct glaciological method were started  
172 on La Mare Glacier in 2003 and detected an average annual mass balance of -0.76  
173 m w.e. y<sup>-1</sup> during the period from 2003 to 2014 (Carturan, [2015](#)[2016](#)). The mass  
174 balance was close to zero in 2013 (-0.06 m w.e.) and was positive for the first time  
175 since the beginning of measurements in 2014 (+0.83 m w.e.).

176 The AVDM3 Rock Glacier (Carturan et al., 2015) is an intact, tongue-shaped rock  
177 glacier characterized by the presence of two lobes. The 0.058 km<sup>2</sup> wide Rock Glacier  
178 (maximum length of 390 m; maximum width of 240 m) faces south-east and is  
179 located at elevations of between 2943 and 3085 m a.s.l. The average slope of the  
180 Rock Glacier is 26°, and the slope of the advancing front is 36°. The activity status of  
181 the AVDM3 Rock Glacier was assessed via repeated geomorphological field surveys  
182 between 2007 and 2014. These surveys revealed the advance of the front of the  
183 southern lobe (Carturan, 2010). The general morphology and the elevation of the  
184 front also suggest that this rock glacier is active (Seppi et al., 2012), and its  
185 permafrost content is further corroborated by spring temperature measurements  
186 (Carturan et al., 2015). Moreover, Bertone (2014) provided the first quantification of  
187 the surface displacement rates of this rock glacier for 2003 to 2013 using ALS data.

188

### 189 **3. Methods**

190 ~~In this section, we briefly describe the ALS data that were used to i) select the ground~~  
191 ~~control points (GCPs) required to scale and georeference the SfM 3D models, ii) co-~~  
192 ~~register the point clouds before producing the DEMs, and iii) validate the~~  
193 ~~photogrammetric results. Then, we describe how the photogrammetric surveys were~~  
194 ~~performed and processed to produce the dense point clouds and DEMs of the La~~  
195 ~~Mare Glacier and AVDM3 Rock Glacier~~

196

#### 197 **3.1 The ALS data**

198 ALS flights of the study area were available for 17 September 2003, 22 September  
199 2013, and 24 September 2014. The technical specifications of the three ALS surveys  
200 are reported in Table 1. To avoid errors due to global shifts or rotations between the  
201 individual DEMs, ~~we automatically co-registered~~ the ALS point clouds were  
202 automatically co-registered using a version of the ICP algorithm (Chen and Medioni,  
203 1991; Besl and McKay, 1992) tailored to topographic point clouds (Glira et al., 2015).  
204 The LiDAR point cloud acquired in 2013 was treated as a reference only for stable  
205 areas outside the glaciers, rock glaciers, snow patches, and geomorphologically  
206 active areas (e.g., landslides, river beds, and debris flows). The 2003 and 2014  
207 LiDAR point clouds were iteratively fitted to the reference point cloud by applying an  
208 affine transformation. The ICP registration of the point clouds produced z-direction  
209 residual values of 0.08 m and 0.11 m for the 2014 and 2003 LiDAR point clouds,  
210 respectively. These accuracies can be assumed to be sufficient for calculating the  
211 annual elevation changes of the glacier and the decadal displacement rate on the  
212 rock glacier.

213 The co-registered point clouds were then converted to DEMs using Natural  
214 Neighbours interpolations. A pixel size of 1 x 1 m was produced for the La Mare  
215 Glacier, whereas a pixel size of 0.5 x 0.5 m was used for the rock glacier, based on  
216 the LiDAR point cloud density (Fig. 2). To evaluate the relative ALS DEM accuracies  
217 after the co-registration, the elevation difference errors of the DEMs were calculated  
218 for the stable areas. The standard deviation from the 2013 ALS DEM was 0.19 m and  
219 0.21 m for the 2014 and 2003 DEM comparisons, respectively.

220

221

## 222 **3.2 The photogrammetric workflow**

### 223 **3.2.1 Field surveys**

224 The terrestrial photogrammetric surveys of the La Mare Glacier were conducted on 4  
225 September 2013 and 27 September 2014, that is, close to the end of the mass  
226 balance year and of ALS flights. The timing of the surveys enabled the calculation of  
227 the annual mass balance of the glacier and ~~the ability~~ to compare the results with the  
228 ALS-based results. On both days, the sky was clear, with almost no cloud cover.

229 To guarantee a safe and easily repeatable survey of the glacier, ~~we avoided directly~~  
230 ~~accessing its surface, instead performing the direct access to its surface was avoided~~  
231 ~~and by performing~~ the survey was performed from a rocky ridge on the north side of  
232 the glacier (Fig. 45). The elevation of the survey ranged from 3100 to 3300 m in 2013  
233 and from 2600 to 3300 m in 2014. The distance from the glacier surface to the  
234 camera positions dictated by the topography ranged between 300 and 2900 m. To  
235 cover the entire glacier surface from these positions, the acquired images were  
236 panoramic, which involved taking a series of photographs rotating the camera from  
237 each individual camera position. In 2013, seven camera positions were used, and 37  
238 photographs were taken with the camera attached to a small tripod to avoid camera  
239 shake. In 2014, the number of camera positions was increased to 21, and 177 photos  
240 were taken freehand (Fig. 3).

241 Both surveys were performed using a SLR Canon EOS 600D. The camera was  
242 equipped with a 25-70 mm zoom lens, which was set to a focal length of 25 mm in  
243 2013 and 35 mm in 2014.

244 The terrestrial photogrammetric survey of the AVDM3 Rock Glacier was performed  
245 on 27 September 2014. In this survey, 198 images were acquired freehand while  
246 walking around and on top of the rock glacier. The survey camera was a CANON  
247 EOS 5D full frame SLR camera equipped with a fixed-focal lens of 28 mm. The  
248 photographs were acquired and saved in RAW format in both surveys.

249

### 250 **3.2.2 Data processing**

251 The ~~latest evolution of photogrammetry is characterized by the combination of the~~  
252 ~~principles of photogrammetry, such as bundle adjustment, and automatic computer~~  
253 ~~vision algorithms, such as feature extraction and feature matching. This~~  
254 photogrammetric approach, ~~called based on Structure from Motion (SfM algorithms),~~  
255 can automatically derive the 3D position of an object in images taken in sequence  
256 calculating the camera parameters (intrinsic and extrinsic) (Hartley and Zissermann,  
257 2004). Dense image matching algorithms are then used to reconstruct the 3D model  
258 of the object as a dense point cloud. Multiple photogrammetric packages  
259 implementing SfM and Multi-View Stereo (MVS) algorithms for dense image  
260 matching exist, and in this work, ~~we used~~ the software PhotoScan Pro (AgiSoft LLC).

261 2010a) was used. Henceforth, ~~we refer to~~ the photogrammetric surveys and results  
262 are referred to using the acronym SfM-MVS.

263 The photo-based reconstruction workflow is summarized in Fig. 4. The key  
264 components of the workflow are 1) acquisition and photograph editing, 2) GCPs  
265 identification, image feature detection, matching and 3D scene reproduction (the  
266 SfM-MVS steps), 3) point cloud processing, (filtering, subsampling and ICP) and 4)  
267 DEM reconstruction.

268 To overcome the significant variability in brightness during the surveys, the RAW  
269 images have been edited to adjust the exposure and contrast in order to retrieve  
270 information from the overexposed (e.g., snow-covered) areas and underexposed  
271 (e.g., shadowed) areas. These editing steps had a positive impact on the number of  
272 image features extracted. The edited images were saved in TIFF format and loaded  
273 in PhotoScan where non-stationary objects (i.e., clouds and shadows), the sky, and  
274 features lying in the distant background have been masked.

275 The camera calibration parameters were calculated using artificial targets prior to the  
276 processing of the photogrammetric surveys (pre-calibrated camera). The intrinsic  
277 parameters were kept constant during the entire SfM processing given the limits of  
278 the camera network geometry and the homogeneous texture of the surveyed terrain.  
279 As additional constraint, the GCPs were included into the SfM process to avoid  
280 instability in the bundle adjustment solution (Verhoeven et al., 2015). The GCPs were  
281 selected as natural features in stable area outside the glacier and rock glacier, and  
282 their coordinates were extracted from the 2013 ALS hillshaded DEM. After the SfM  
283 step, the geo-referenced dense point cloud was reconstructed by the MVS algorithm,  
284 using the 'mild' smoothing filter to preserve as much spatial information as possible  
285 (AgiSoft LLC., 2010b).

286 To reduce the noise and outliers generated during the dense matching reconstruction  
287 (Bradley et al., 2008; Nilosek et al., 2012), an initial filtering was performed in  
288 PhotoScan to manually remove the outliers. Further denoising was applied to the  
289 dense point clouds exported from PhotoScan, using a specific tool to treat the point  
290 clouds. To obtain a uniform spatial distribution of the points, the photogrammetric  
291 point clouds (much denser than the ALS point clouds), were down-sampled to 20 cm  
292 for the glacier and 10 cm for the rock glacier. Following the same procedure used for  
293 the ALS data, the ICP algorithm (OpalsICP, TU ~~Vienna~~Wien) was applied to co-  
294 register the point clouds in the stable area outside the glacier and rock glacier, using



295 the 2013 ALS point cloud as a reference. The co-registered point clouds were then  
296 converted to DEMs, using the Natural Neighbours interpolation and the pixel sizes of  
297 the ALS DEMs (i.e., 1 x 1 m for the glacier and 0.5 x 0.5 m for the rock glacier). The  
298 data acquisition settings and processing results of the photogrammetric surveys are  
299 summarized in Table 2.

300

### 301 3.3 Analyses

302 The accuracy of the photogrammetric DEMs was assessed ~~to calculate~~ calculating  
303 the mean, the mean of the absolute values and the standard deviation ( $\sigma$ ) of the  
304 elevation differences (DEM of Difference, DoD) between SfM-MVS DEMs and ALS  
305 DEMs, using the latter as a reference dataset. For both surveyed areas, the primary  
306 factors controlling the quality of the photogrammetric ~~results~~ DEMs (i.e., camera-  
307 object distance, slope and angle of incidence, camera network geometry, surface  
308 texture and shadows) were evaluated in terms of DEM accuracy and spatial  
309 resolution. The obtained results were compared to analysis of the theoretical error  
310 propagation behaviour of the error as a function of the depth ( $\sigma_d$ ) direction (camera-  
311 object distance), was calculated using the following formulation:

$$312 \quad \sigma_d = m_B \cdot \frac{D}{B} \cdot \sigma_i \quad (1)$$

313 where  $m_B$  represents the image scale ( $D / \text{focal length}$ );  $D$  is the depth (camera-object  
314 distance);  $B$  is the baseline and  $\sigma_i$  is the measured accuracy in the image space.

315 After the accuracy assessments, we investigated the suitability of using the terrestrial  
316 photogrammetric surveys to calculate the annual mass balance of the glacier and the  
317 elevation change and ~~the~~ surface displacement rates of the rock glacier, comparing  
318 the results with those obtained from ALS surveys. The mass balance and elevation  
319 changes were calculated differencing multitemporal DEMs.

320 The geodetic mass balance was calculated from the total volume change  $\Delta V$  ( $\text{m}^3$ )  
321 between two survey dates: using the following relation

$$322 \quad V = \overline{\Delta z} \cdot A \quad (2)$$

323 where  $\overline{\Delta z}$  is the average elevation change between two DEMs over the area  $A$  of the  
324 glacier. The area-averaged net geodetic mass balance in metres of water equivalent  
325 per year ( $\text{m w.e. y}^{-1}$ ) was calculated as:

$$\dot{M} = \frac{\Delta V \cdot \rho}{A} \quad (3)$$

where  $\rho$  is the mean density. The area  $A$  of the glacier between the two surveys did not change. The mean density was obtained by a fractional area-weighted mean, assigning  $900 \text{ kg/m}^3$  for the ablation area (Huss, 2013) and  $530 \text{ kg/m}^3$  for the accumulation area, as directly measured in a snowpit. The resulting weighted mean density was  $600 \text{ kg/m}^3$ . In the mass balance calculations, both raw  $\overline{\Delta z}$  values and corrected  $\overline{\Delta z}$  values were used to account for the mean errors in the stable areas outside the glacier, as reported in Table 3. Other processes –like ice fluxes, and varying snow density and re-freezing of melt water were assumed to be negligible for the not taken into account to estimate calculation of the annual geodetic mass balance.

The horizontal surface displacements rates of the AVDM3 rock glacier were estimated by means of manual detection of features on the hillshaded DEMs. a manual measurement of the displacement of single boulders identified in the hillshaded DEMs. Several points were also located outside the rock glacier to assess the accuracy of the surface velocity determinations. Displacements in the horizontal plane were analysed instead of 3D displacements, which are affected by surface elevation changes (Isaksen et al., 2000).

±

## 4. Results

### 4.1 Accuracy assessment on the area of La Mare Glacier

The mean elevation difference between the SfM-MVS DEM from 4 September 2013 (Fig. 5a) and the ALS DEM from 22 September 2013 (Fig. 2b), evaluated in the common stable area outside the glacier, was  $-0.42 \text{ m}$  ( $\sigma = 1.72 \text{ m}$ ). The same calculation between the SfM-MVS DEM from 27 September 2014 (Fig. 5b) and the ALS DEM from 24 September 2014 (Fig. 2a) yielded a mean value of  $0.03 \text{ m}$  ( $\sigma = 0.74 \text{ m}$ ). In this area, the mean difference between the 2014 and 2013 SfM-MVS DEMs is  $0.38 \text{ m}$  ( $\sigma = 1.73 \text{ m}$ ), and the mean difference between the respective ALS DEMs is  $-0.09 \text{ m}$  ( $\sigma = 0.29 \text{ m}$ , Table 3).

356 These results show that the photogrammetric survey conducted in 2014, using a  
357 higher number of camera positions and photographs and a slightly longer focal  
358 length, provided a significant improvement compared to the survey of 2013. In  
359 addition to the higher  $\sigma$ , the 2013 SfM-MVS DEM has a residual average bias of -  
360 0.42 m, which must be taken into account in the glacier mass balance calculations.

361 Table 3 ~~also~~ presents the same statistics for the area of the glacier. However, given  
362 that in 2013 the ablation was not negligible between the photogrammetric survey of 4  
363 September and the ALS survey of 22 September, the comparison between SfM-MVS  
364 and ALS of the same year is meaningful only in 2014, with a mean difference of 0.23  
365 m ( $\sigma = 0.65$  m). The comparison of the two ALS DEMs of 2014 and 2013 yields a  
366 mean difference of 1.30 m for the glacier, attributable to the positive mass balance  
367 experienced by the glacier in that time period (+0.83 m w.e., Carturan, ~~2015~~2016).

368 The spatial distribution of the elevation difference between the SfM-MVS and ALS  
369 DEMs surveyed at the same times (Fig. 6 and 7) suggests that the most problematic  
370 areas for photogrammetric reconstructions are those that are far from the camera  
371 positions, steep, and covered by fresh snow. Certain outliers can be observed in  
372 steep areas outside the glaciers, even after filtering, but they likely have no influence  
373 on the glacier, where the slope is much lower.

374 The factors controlling the quality of the photogrammetric DEMs were investigated in  
375 detail uUsing the SfM-MVS DEM from 27 September 2014, which has a higher  
376 spatial coverage than that of 2013 and is almost contemporaneous with the ALS  
377 DEM from 24 September 2014 (which means negligible ablation and accumulation on  
378 the glacier), ~~we investigated in detail the factors controlling the quality of the~~  
379 ~~photogrammetric DEMs.~~

380 As expected, the standard deviation of elevation differences between the 2014 SfM-  
381 MVS and ALS DEMs is proportional to slope but remains lower than 1 m up to 40° on  
382 the glacier and up to 60° in the area outside it (Fig. 8). Grouping the data for slope  
383 classes of 10 degrees and excluding classes with less than 1000 grid cells, it was  
384 possible to calculate a strong correlation between the absolute value of the elevation  
385 difference and the slope (R = 0.86 both inside and outside the glacier, significant at  
386 the 0.05 level). A rapid increase in the error is observed for the highest slope classes,  
387 which represent a very small part of the investigated area. For the glacier, only 1% of  
388 the area has a slope higher than 40°. The mean elevation difference is around zero  
389 for most of the low- and middle-slope classes, with the exception of the 0-10° class

390 inside the glacier, where a mean value of 0.41 m ( $\sigma = 0.44$  m) was calculated.  
391 Interestingly, the majority of this slope class lies in a flat area of the glacier at 3200-  
392 3300 m a.s.l. and is covered by fresh snow, which has poor texture. In addition, this  
393 zone has an unfavourable line of sight from the camera positions.

394 ~~We therefore investigated the role of the incidence angle between the line of sight~~  
395 ~~of the camera and the photographed object (vector normal to the surface), was~~  
396 ~~investigated by analysing the mean angles calculated from five representative~~  
397 ~~camera locations at different elevations. The analysis was performed for the glacier~~  
398 ~~area, where most of the mean incidence angles ranges between 70° and 90° (75%,~~  
399 ~~Figure 9a). As Figure 9a shows, more than 80% of the incidence angles in single~~  
400 ~~pixels range between 70° and 90°. The scatterplot Figure (Fig 9c) of elevation~~  
401 ~~differences between the 2014 SfM-MVS and ALS DEMs and versus the mean~~  
402 ~~incidence angles calculated for each every pixel shows no statistically significant~~  
403 ~~relationship ( $R^2 = 0.04521$ ). between incidence angle and elevation~~  
404 ~~difference. However, by analysing this relationship for intervals classes of incidence~~  
405 ~~angle, and considering the mean of the absolute value of elevation differences in~~  
406 ~~absolute value and the classes with more than 1000 pixels, yields a correlation~~  
407 ~~coefficient  $R = 0.95$  (significant at the 0.05 level), confirming the conclusions~~  
408 ~~reached by Piermattei et al. (2015). Contrary to what was speculated, high mean and~~  
409 ~~standard deviation values were obtained for low (i.e., theoretically favourable)~~  
410 ~~incidence angles, which correspond to areas with high slope. Instead, low and~~  
411 ~~approximately constant low standard deviation values were obtained for high~~  
412 ~~incidence angles. These results suggest that, in our case study, the accuracy of the~~  
413 ~~SfM-MVS DEMs is influenced more by the slope than by the incidence angle.~~

414 ~~Because the redundancy of the observations, that is that means the number of~~  
415 ~~camera that view cameras that views the same points on the glacier, is a factor that~~  
416 ~~influences the quality of the photogrammetric results, a viewshed analysis was~~  
417 ~~carried out (Fig. 9d). The results showed anti-correlation between the absolute value~~  
418 ~~of elevation difference and the number of cameras viewing reconstructed pixels (Fig.~~  
419 ~~9e), yielding a coefficient of correlation of -0.63, which is significant at the 0.05 level.~~

420 ~~The effect of the~~ Because the camera-object distance (i.e., depth, ) strongly  
421 influences the photogrammetric accuracy (Gómez-Gutiérrez et al., 2014), we  
422 evaluated its effect was evaluated by calculating the mean and standard deviation of  
423 the elevation difference between the 2014 SfM-MVS and ALS DEMs, clustering the

424 pixels in 200 m distance classes from a camera position at the centre of the array  
425 displayed in Figure 4b. The relationship between error and depth is clearer for the  
426 glacier area (Fig. 10a), whereas in the surrounding area, the error appears to be  
427 more influenced by the variability of the slope angle (Fig. 10b).

428 ~~The obtained results were compared to the theoretical behaviour of the error~~  
429 ~~according to the Eq. 1, as a function of the depth ( $\sigma_d$ ), as calculated using the~~  
430 ~~following formulation:~~

$$431 \sigma_d = m_B \cdot \frac{D}{B} \cdot \sigma_i, \quad (1)$$

432 ~~where  $m_B$  represents the image scale ( $D / \text{focal length}$ );  $D$  is the depth (camera-object~~  
433 ~~distance);  $B$  is the baseline and  $\sigma_i$  is the measured accuracy in the image space.~~

434 The theoretical  $\sigma_d$  was calculated using Eq. 1 for each class of distance, considering  
435 a mean baseline of 400 m and an accuracy in the image space of 0.40 pixel, which is  
436 the reprojection error after bundle adjustment computations. Another quantification of  
437 the error as a function of the depth was obtained, for comparison purposes, by  
438 multiplying the Ground Sample Distance (GSD) (which increases with depth) by the  
439 reprojection error provided by PhotoScan for the Ground Control Points. Figure 10c  
440 shows that, on the glacier, the accuracy calculated from the DoD matches quite well  
441 the ‘theoretical’ calculations up to a depth of 1900 m. Beyond this distance, the  
442 detected error increases faster than in theory, likely due to the increasing coverage of  
443 fresh snow, which affects the image texture and decreases the accuracy.

444 ~~We then investigated the~~ accuracy of photogrammetric reconstructions for the  
445 different substrata was then evaluated. ~~The whose~~ spatial distribution of each  
446 substrata ~~substratum~~ was outlined on the orthophoto exported from PhotoScan.  
447 Debris, ice and firn display similar accuracy, with median values of elevation  
448 difference between the 2014 SfM-MVS and ALS-based DEMs close to zero and  
449 interquartile ranges of the same magnitude. Conversely, the area covered by fresh  
450 snow, which is also the area with greater depth, shows prevailing positive  
451 differences, a median value of 0.48 m and a much higher standard deviation ( $\sigma =$   
452 0.82 m).

453 The texture of the surface also influences the point density distribution and the spatial  
454 coverage of the reconstructed area. A lower value of the point density was obtained

455 for fresh snow (4 pts m<sup>-2</sup>). Increasing point densities were obtained for firn, ice and  
456 debris (10, 13 and 15 pts m<sup>-2</sup>, respectively).

457 The spatial coverage in the fresh snow area was 75%, whereas it was 93% in the  
458 rest of the glacier. Excluding the areas not visible from the camera position and  
459 occlusions imposed by the topography, the spatial coverage in the fresh snow area  
460 was 82% and 98% in the remaining part.

461 The point density is also affected by the depth, elevation and slope (Fig. 12). Due to  
462 the GSD, the average point density decreases with depth, which in our case is also  
463 proportional to the elevation. On the glacier, the point density decreases more rapidly  
464 than in the surrounding area for elevations between 3100 and 3300 m a.s.l., due to  
465 the poor texture in this snow-covered flat area. Increasing densities with slope, up to  
466 70-80°, are observed and likely result from more favourable incidence angles, which  
467 do not however guarantee high accuracy, as noted earlier (Fig. 9). Considering the  
468 entire reconstructed surface, the point density was higher in the area surrounding the  
469 glacier than on it (12 pts m<sup>-2</sup> vs. 8 pts m<sup>-2</sup>, respectively).

470

#### 471 **4.2 Accuracy assessment in the area of the AVDM3 Rock Glacier**

472 The 2014 terrestrial photogrammetric survey of the AVDM3 Rock Glacier provided a  
473 good spatial coverage (83%) of high-resolution terrain data (Fig. 13). The spatial  
474 distribution of the elevation difference between the contemporaneous SfM-MVS and  
475 ALS DEMs shows the existence of areas with both positive and negative values (Fig.  
476 14). The average elevation difference is 0.02 m on the rock glacier ( $\sigma = 0.17$ ) and  
477 0.05 in the surrounding areas ( $\sigma = 0.31$  m, Tab. 5).

478 Similar to the La Mare Glacier area, the accuracy decreases with increasing slope in  
479 the rock glacier area. The standard deviation of the average elevation difference  
480 between the SfM-MVS and ALS DEMs is less than 0.20 m up to 40°. In the area  
481 surrounding the rock glacier, the error increases faster with slope because steep  
482 areas coincide with shaded areas and (because the images were acquired in the  
483 afternoon) high solar zenith angles. As suggested by Gómez-Gutiérrez et al., (2014),  
484 ~~we calculated~~ the relationship between the quality of the photogrammetric DEM and  
485 the amount of shadowed-lighted areas in the photographs was calculated, using a  
486 hillshaded model that was calculated by simulating the position of the sun in the sky  
487 (azimuth and zenith angles) during the survey. As shown in Figure 16, larger errors

488 occur in shadowed areas and smaller errors in well-lit areas, even if the largest  
489 differences in accuracy can be observed outside rather than on the rock glacier.

490

### 491 4.3 Glacial and periglacial processes

#### 492 4.3.1 Mass balance ~~calculations of on~~ La Mare Glacier

493 Due to abundant solid precipitation during the accumulation season and low ablation  
494 rates during the summer (the glacier was snow-covered above ~3000-3100 m a.s.l.),  
495 the mass balance of the La Mare Glacier was positive in the 2013-14 hydrological  
496 year for the first time since the beginning of measurements in 2003. ~~At the end of the~~  
497 ~~ablation season, the Equilibrium Line Altitude (ELA) was at 3012 m a.s.l., and the~~  
498 ~~Accumulation Area Ratio (i.e., the ratio between the accumulation area and the total~~  
499 ~~area, AAR) was 0.86.~~ According to the direct glaciological method, the annual mass  
500 balance was +0.83 m w.e. (Carturan, ~~2015~~2016).

501 ~~We compared mass balance estimates obtained was calculated according to the Eq.~~  
502 ~~3 with the geodetic method based on for the SfM-MVS and ALS DEMs acquired in~~  
503 ~~2013 and 2014 and the results was compared. The geodetic mass balance was~~  
504 ~~calculated from the total volume change  $\Delta V$  ( $m^3$ ) between the two survey dates:~~

$$505 V = \overline{\Delta z} \cdot A \quad (2)$$

506 ~~where  $\overline{\Delta z}$  is the average elevation change between two DEMs over the area  $A$  of the~~  
507 ~~glacier. The area-averaged net geodetic mass balance in metres of water equivalent~~  
508 ~~per year ( $m \text{ w.e. } y^{-1}$ ) was calculated as~~

$$509 \dot{M} = \frac{\Delta V \cdot \rho}{A} \quad (3)$$

510 ~~where  $\rho$  is the mean density. The area  $A$  of the glacier between the two surveys did~~  
511 ~~not change. The mean density was obtained by a fractional area-weighted mean,~~  
512 ~~assigning  $900 \text{ kg/m}^3$  for the ablation area (Huss, 2013) and  $530 \text{ kg/m}^3$  for the~~  
513 ~~accumulation area, as directly measured in a snowpit. The resulting weighted mean~~  
514 ~~density was  $600 \text{ kg/m}^3$ . In the mass balance calculations, we used both raw  $\overline{\Delta z}$~~   
515 ~~values and corrected  $\overline{\Delta z}$  values to account for the mean errors in the stable areas~~  
516 ~~outside the glacier, as reported in Table 3.~~

517 As shown in Table 4, the geodetic mass balance estimates using only ALS data do  
518 not differ significantly for either the entire glacier or the sub-areas covered by the  
519 photogrammetric surveys of 2013 and 2014 (88% and 93%, respectively). The

520 estimates range between 0.85 and 0.88 m w.e for the raw data and between 0.90  
521 and 0.94 m w.e. for the corrected data. The geodetic mass balance calculations  
522 using only photogrammetric data yield a raw value of 1.09 m w.e. and a corrected  
523 value of 0.87 m w.e. Using the 2014 SfM-MVS, which has a higher quality than the  
524 2013 ALS DEM, yields a raw value of 0.98 m w.e. and a corrected value of 1.02 m  
525 w.e. Area-averaged estimates of the geodetic mass balance from photogrammetric  
526 data are very close to the estimates from ALS data and from the direct method and  
527 are closer still if the mean DEM error in the stable areas outside the glacier is  
528 subtracted from the raw average elevation differences. The spatial distribution and  
529 magnitude of elevation change is also well captured by the terrestrial  
530 photogrammetry (Fig. 17 and 18), even if, as already noted in the previous section,  
531 problematic areas are present in the upper part of the glacier, which was covered by  
532 fresh snow, especially in the 2013 SfM-MVS survey.

533

#### 534 **4.3.2 Surface changes and velocities of the AVDM3 Rock Glacier**

535 The spatial distribution and the mean value of elevation change on the surface of the  
536 AVDM3 Rock Glacier were calculated differencing the available SfM-MVS and ALS  
537 DEMs. Table 5 shows that, according to the ALS data, there was a prevailing  
538 lowering of the surface in the period from 2003 to 2014. Taking into account the  
539 average residual bias in the stable area outside the rock glacier, the average  
540 lowering rates of the rock glacier surface were 1.5 cm  $y^{-1}$  in the period from 2003 to  
541 2013, and 2 cm in the year 2013-14. Comparing the SfM-MVS DEM of 2014 with the  
542 ALS DEMs of 2013 and 2003 and accounting for the mean bias outside the rock  
543 glacier, we obtained slightly higher lowering rates of 2.2 cm  $y^{-1}$  from 2003 to 2013  
544 and 5 cm from 2013 to 2014. As expected on the basis of the accuracy assessment  
545 (Section 4.2), the decadal lowering rates calculated from the SfM-MVS DEM are in  
546 closer agreement with those calculated from ALS data than the single-year  
547 calculations. The same can be observed for the spatial distribution of the elevation  
548 changes (Fig. 19), which shows a prevailing thinning in the upper and middle part of  
549 the rock glacier and a thickening of the two advancing lobes.

550 ~~Based on these results, we compared the surface displacement rates (based on~~  
551 ~~photogrammetric and ALS data) for the period from 2003 to 2014. We used by a~~  
552 ~~manual measurements of the displacement of single boulders identified in the~~



553 ~~hillshaded DEMs. Several points were also located outside the rock glacier to assess~~  
554 ~~the accuracy of the surface velocity determinations.~~

555 Figure 20 shows that the fastest moving areas in the period from 2003 to 2014 ~~are~~  
556 ~~were~~ the two frontal lobes, which also featured the greatest elevation changes. Table  
557 6 shows that the SfM-MVS and ALS data produced very similar surface velocities for  
558 the three sub-areas (each with homogeneous displacement) into which the rock  
559 glacier can be divided. Outside the rock glacier, the photogrammetric method  
560 exhibited a slightly lower accuracy compared to the ALS, but no systematic shift of  
561 the different DEMs was found.

562

## 563 **5. Discussion**

### 564 5.1 Data processing and accuracy assessments

565 The results of our terrestrial photogrammetry applications on the La Mare Glacier and  
566 on the AVDM3 Rock Glacier demonstrate that it is possible to reliably quantify the  
567 investigated glacial and periglacial processes by means of a quick and safe survey  
568 that was conducted on a single day using cheap, light and easy-to-use hardware.  
569 Moreover, time-consuming and unsafe direct access to the glacier surface was not  
570 required.

571

572 ~~I~~ However, the data processing times were significantly longer. For a single operator,  
573 the processing time is approximately 10 days. The most labour-intensive and time-  
574 consuming tasks were the pre-processing steps i.e., masking of the photos,  
575 identification of reference points from the LiDAR DEM and then in the images, and  
576 processing of the images (the MVS step is particularly computationally intensive),  
577 which is directly related to the resolution and the number of photographs uploaded  
578 and the computer performance. Several steps required a certain degree of  
579 subjectivity, e.g., the identification of the GCPs. However, due to the high automatism  
580 of the image processing, the level of expertise is considerably lower than for LiDAR  
581 and traditional photogrammetry.

582 On the La Mare Glacier, the area-averaged estimates of the 2013-14 geodetic mass  
583 balance from ALS and photogrammetric data were almost identical (0.91 and 0.87 m  
584 w.e., respectively) and close to the mass balance calculated from the direct

585 glaciological method (0.83 m w.e.). The differences are well within the uncertainty of  
586 the direct mass balance estimates, which ~~was quantified in 0.26~~has been quantified  
587 ~~as approximately  $\pm 0.2$  m w.e.  $y^{-1}$  by previous studies (Cogley and Adams, 1998;~~  
588 ~~Cogley, 2009)~~Carturan (2016). These results confirm that the good results obtained  
589 by Piermattei et al., (2015) on the small Montasio Glacier, in the Julian Alps, can also  
590 be replicated on larger glaciers with different morphologies and characteristics.  
591 Because the AVDM3 Rock Glacier exhibited quite slow annual deformation and  
592 creep, we were able to calculate reliable displacement rates and area-averaged  
593 surface elevation changes only on a multi-year (in our case, decadal) time scale. This  
594 result confirms the findings of Gómez-Gutiérrez et al. (2014), who applied a similar  
595 method to the Corral del Veleta Rock Glacier in the Sierra Nevada (Spain).  
596 Our results are promising, despite the limitations of the adopted method, which  
597 include i) the location of GCPs on natural targets outside the investigated glacier/rock  
598 glacier, ii) the presence of areas with deep shadows and changes in the light during  
599 the survey, iii) the presence of fresh snow in the upper and middle part of the glacier,  
600 and iv) the high camera-object distance in the glacier application.  
601 In general terms, the photo-based accuracy is related to the image feature extraction,  
602 feature matching (in both the SfM and MVS steps), and scale definition (Bemis et al.,  
603 2014). A low accuracy in these steps, caused for example by poor camera network  
604 geometry, can generate model distortion and reduce the ability to identify unique  
605 corresponding features in overlapping images (Wackrow and Chandler, 2011;  
606 Dall'Asta et al., 2015b, Favalli et al., 2012; James and Robson, 2012; 2014;  
607 Hosseinaveh et al, 2014; Micheletti et al., 2014; Nocerino et al., 2014). In our case  
608 studies, among the various aspects analysed, the spatial variability of the accuracy of  
609 the photogrammetric DEMs is related to the camera-object distance, the presence of  
610 fresh snow with low contrast, the changing illumination during the survey and the  
611 occurrence of shadows. The increasing error with increasing terrain slope suggests  
612 the persistence of a small shift in the reconstructed DEMs. This shift, however does  
613 not affect the areal estimates of mass balance and elevation change, given that the  
614 vast majority of the glacier and rock glacier areas feature small or moderate slope  
615 angles. For both the glacier and the rock glacier, the spatial coverage of the  
616 reconstructed areas was not complete.~~, we have not obtained complete spatial~~  
617 ~~coverage was obtained.~~ In the glacier surveys, the problematic areas were those not  
618 visible from the camera positions and those covered by fresh snow and far from the

619 viewpoints. In the rock glacier, certain areas were not reconstructed due to the rock  
620 glacier's complex morphology and in particular to the presence of ridges, furrows and  
621 counterslopes.

622

## 623 5.2 RecommendationsPossible improvements of the SfM-MVS approach

624 ~~Our~~The accuracy assessments confirm that the ALS data still provide results with  
625 somewhat higher accuracies (Tabs. 3 and 5, Figs. 6 and 14) but with much higher  
626 costs and demanding logistics than the SfM-MVS approach. However, the SfM-MVS  
627 method has the potential to provide a significantly higher spatial resolution (Debella-  
628 Gilo and Kaab, 2011; Piermattei et al., 2015) and temporal resolution due to its  
629 significantly lower costs. Moreover, the photogrammetric reconstructions still have  
630 room for improvement, as demonstrated by the better results achieved from the 2014  
631 survey of the glacier area compared to those from 2013. This improvement resulted  
632 from a higher number of photographs and improved camera network geometry.

633 Many of the limitations described above can be overcome by introducing  
634 modifications to the terrestrial photogrammetric survey strategy. For the rock glacier  
635 survey, shorter baselines are recommended to ensure greater spatial coverage, high  
636 image similarity and good matching performance (Wenzel et al., 2013). GCPs, for  
637 example, could be placed on the surface of the glaciers and rock glaciers to reduce  
638 the model distortions (Bemis et al., 2014) and generate surveys with much higher  
639 accuracies via, for example, the use of dGPS (Dall'Asta et al., 2015a).

640 The use of ~~Unmanned Aerial Vehicles (UAVs)~~ could solve the problem of excessive  
641 camera-object distances and the issue of missing areas due to inaccessibility.  
642 However, these alternatives imply increased costs, more troublesome logistics,  
643 greater expertise, and ultimately longer survey times. In addition, they also require  
644 directly accessing unsafe or difficult to reach areas, both to place targets and to move  
645 UAVs among study areas that exceed their operational range (Bühler et al., 2014).  
646 Therefore, the best balance must be found between simplicity, safety, costs and  
647 accuracy for each photogrammetric application based on the final objectives and on  
648 the available human and economic resources.

649

## 650 **6. Conclusions**

651 In this paper, we investigated the applicability of the SfM-MVS approach for  
652 monitoring glacial and periglacial processes in a catchment of the Ortles-Cevedale  
653 Group (Eastern Italian Alps), validating our results using ALS DEMs as benchmarks.  
654 The ground surveys were conducted on foot and were intentionally planned to be as  
655 quick and easy as possible. ~~We surveyed~~ the 2.1\_-km<sup>2</sup> La Mare Glacier and the  
656 neighbouring AVDM3 Rock Glacier ~~were surveyed~~ in one day using only a consumer-  
657 grade SLR camera without the setup of artificial targets.

658 The accuracy of the photogrammetric DEMs, evaluated as the mean and standard  
659 deviation of the elevation difference in a stable area between the SfM-MVS DEM and  
660 the reference ALS DEM, was  $-0.42 \text{ m} \pm 1.72 \text{ m}$  and  $0.03 \text{ m} \pm 0.74 \text{ m}$  for the 2013 and  
661 2014 surveys, respectively. The SfM-MVS DEM accuracy of the reconstructed rock  
662 glacier surface acquired in 2014 was estimated to be  $0.02 \text{ m} \pm 0.17 \text{ m}$ .

663 The SfM-MVS geodetic mass balance estimates for the La Mare Glacier were in  
664 good agreement with the calculations from the contemporary ALS data and with the  
665 results of the direct glaciological method, confirming a positive mass balance of  
666 approximately 0.9 m w.e. in the 2013-14 hydrological year. In the rock glacier, the  
667 ~~expeditious~~ survey produced a good spatial coverage of the photogrammetric DEM  
668 and a reliable calculation of the multi-year surface changes and displacement rates.  
669 For rock glacier applications, particularly for slow-moving ones such as AVDM3,  
670 single-year assessments of elevation change and surface velocities require the setup  
671 of artificial targets and GCPs to obtain the accuracy required to detect such slow  
672 processes.

673 The simplicity of the ground surveys and the physical characteristics of the analysed  
674 alpine terrain were the main factors influencing the tested approach. In particular, we  
675 refer to the use of natural targets as GCPs, the occurrence of shadowed areas and  
676 lighting changes during the surveys, the presence of fresh snow in the upper part of  
677 the glacier (which reduced the contrast), and the sub-optimal camera network  
678 geometry and long camera-object distances imposed by the morphology and  
679 accessibility of the study area.

680 In consideration of the factors that spatially control the accuracy of the SfM-MVS  
681 DEMs, there remains room for significant improvements, e.g., using ~~UAVs~~ aerial  
682 platform and/or placing artificial targets surveyed by dGPS. Further research is  
683 therefore needed to i) find technical solutions to overcome the major limitations of the  
684 SfM-MVS approach in such remote areas and ii) achieve the optimal balance

685 between the simplicity and low cost of this approach and the accuracy required for  
686 each specific application.

687

## 688 **Acknowledgments**

689 This study was funded by the Italian MIUR Project (PRIN 2010-11): 'Response of  
690 morphoclimatic system dynamics to global changes and related geomorphological  
691 hazards' (local and national coordinators G. Dalla Fontana and C. Baroni). The  
692 authors would like to thank Philipp Glira from the TU of Wien for his precious  
693 contribution to the LiDAR data processing. The comments and suggestions from  
694 Susan Conway, Álvaro Gómez-Gutiérrez and an anonymous Reviewer have been  
695 useful for the improvement of the manuscript.

696

## 697 **References**

698 ~~Abermann, J., Fischer, A., Lambrecht, A., and Geist, T.: On the potential of very high-~~  
699 ~~resolution repeat DEMs in glacial and periglacial environments, The Cryosphere, 4,~~  
700 ~~53–65, doi:10.5194/tc-4-53-2010, 2010.~~

701 AgiSoft LL C: AgiSoft PhotoScan Professional Edition. Version 1.1.2, available at:  
702 <http://www.agisoft.ru/products/photoscan/> (last access: 18 January 2015), 2010a.

703 AgiSoft LL C: AgiSoft PhotoScan User-manuals Version 1.0, available at:  
704 [http://www.agisoft.com/pdf/photoscan-pro\\_1\\_1\\_en.pdf](http://www.agisoft.com/pdf/photoscan-pro_1_1_en.pdf) (last access: 15 May 2015),  
705 2010b.

706 ~~Aguilar, F. J. and Mills, J.: Accuracy assessment of lidar-derived digital elevation~~  
707 ~~models, Photogramm. Rec., 23, 148–169, 2008.~~

708 ~~Ahn, Y. and Box, J., E.: Glacier velocities from time-lapse photos: technique~~  
709 ~~development and first results from the Extreme Ice Survey (EIS) in Greenland. J.~~  
710 ~~Glaciol., 56, 723–734, 2010.~~

711 ~~Baltsavias, E. P., Favey, E., Bauder, A., Bosch, H., and Pateraki, M.: Digital surface~~  
712 ~~modelling by airborne laser scanning and digital photogrammetry for glacier~~  
713 ~~monitoring, Photogramm. Rec., 17, 243–273, doi:10.1111/0031-868X.00182, 2001.~~

714 Bemis, S., Micklethwaite, S., and Turner, D.: Ground-based and UAV-Based  
715 photogrammetry: a multi-scale, high-resolution mapping tool for Structural Geology  
716 and Paleoseismology. *J Struct Geol.*, 69, 163–178, doi:10.1016/j.jsg.2014.10.007,  
717 2014.

718 Bertone, A.: Misure di spostamento dei rock glacier con l'uso di feature tracking  
719 applicato a DTM multitemporali, BSc Thesis, Department of Earth and Environmental  
720 Sciences, University of Pavia, Pavia, Italy, 63 pp., 2014.

721 Besl, P. J. and McKay, N. D.: Method for registration of 3-D shapes, in: Proceedings  
722 of the International Society for Optics and Photonics IEEE Transactions on Pattern  
723 Analysis and Machine Intelligence, 1611, 586–606, 1992.

724 Bradley, D., Boubekur, T., and Heidrich, W.: Accurate multi-view reconstruction  
725 using robust binocular stereo and surface meshing, in: IEEE Conference on  
726 Computer Vision and Pattern Recognition, Anchorage, AK, USA, 1–8, 2008.

727 ~~Bühler, Y. and Graf, C.: Sediment transfer mapping in a high-alpine catchment using~~  
728 ~~airborne LiDAR. GRAF, C.(Red.) Mattertal – ein Tal in Bewegung, Publikation zur~~  
729 ~~Jahrestagung der Schweizerischen Geomorphologischen Gesellschaft, 29 June–1~~  
730 ~~July 2011, Eidg. Forschungsanstalt WSL, St. Niklaus, Birmensdorf, Switzerland, 113–~~  
731 ~~124, 2013.~~

732 Bühler, Y., Marty, M., Egli, L., Veitinger, J., Jonas, T., Thee, P., and Ginzler, C.:  
733 Spatially continuous mapping of snow depth in high alpine catchments using digital  
734 photogrammetry, *The Cryosphere Discuss.*, 8, 3297–3333, doi:10.5194/tcd-8-3297-  
735 2014, 2014.

736 Carturan, L.: Climate change effects on the cryosphere and hydrology of a high-  
737 altitude watershed, PhD thesis, Department of Land, Environment, Agriculture and  
738 Forestry, University of Padova, Padova, Italy, 2010.

739 Carturan, L.: Replacing monitored glaciers undergoing extinction: a new  
740 measurement series on La Mare Glacier (Ortles-Cevedale, Italy) Starting new mass  
741 balance observations close to decaying monitored glaciers: La Mare Glacier (Ortles-  
742 Cevedale, Italian Alps), *J. Glaciol.*, in preparation review, 20152016.

743 Carturan, L., Cazorzi, F., and Dalla Fontana, G.: Enhanced estimation of glacier  
744 mass balance in unsampled areas by means of topographic data, *Ann. Glaciol.*, 50,  
745 37–46, 2009.

746 Carturan, L., Baldassi, G., Bondesan, A., Calligaro, S., Carton, A., Cazorzi, F., Dalla  
747 Fontana, G., Francese, R., Guarnieri, A., Milan, N., Moro, D., Tarolli, P.: Current  
748 behavior and dynamics of the lowermost Italian glacier (Montasio Occidentale, Julian  
749 Alps), *Geografiska Annaler: Series A, Physical Geography*, 95, 79–96, 2013.

750 Carturan, L., Baroni, C., Carton, A., Cazorzi, F., Fontana, G. D., Delpero, C., and  
751 Zanoner, T.: Reconstructing Fluctuations of La Mare Glacier (Eastern Italian Alps) in  
752 the Late Holocene: new Evidence for a Little Ice Age Maximum Around 1600 AD.  
753 *Geografiska Annaler: Series A, Physical Geography*, 96, 287–306, 2014.

754 Carturan, L., Zuecco, G., Seppi, R., Zanoner, Z., Borga, M., Carton, A., and Dalla  
755 Fontana, G.: Catchment-scale permafrost mapping using spring water  
756 characteristics, *Permafrost Periglac.*, in press, [doi: 10.1002/ppp.1875](https://doi.org/10.1002/ppp.1875), 2015.

757 Chen, Y. and Medioni, G.: Object modeling by registration of multiple range images,  
758 in: *Proceedings, IEEE International Conference on Robotics and Automation*, 9–11  
759 April, Sacramento, CA, USA, 10, 145–155, 1991.

760 ~~Clapuyt, F., Vanacker, V., and Van Oost, K.: Reproducibility of uav-based earth  
761 topography reconstructions based on structure-from-motion algorithms,  
762 *Geomorphology*, doi:10.1016/j.geomorph.2015.05.011, 2015.~~

763 ~~Cogley, J. G.: Geodetic and direct mass-balance measurements: comparison and  
764 joint analysis, *Ann. Glaciol.*, 50, 96–100, 2009.~~

765 ~~Cogley, J. G. and Adams, W. P.: Mass balance of glaciers other than the ice sheets,  
766 *J. Glaciol.*, 44, 315–325, 1998.~~

767 ~~Colucci, R. R., Forte, E., Boccali, C., Dossi, M., Lanza, L., Pipan, M., and Guglielmin,  
768 M.: Evaluation of internal structure, volume and mass of glacial bodies by integrated  
769 LiDAR and ground penetrating radar surveys: the case study of Canin Eastern  
770 Glacieret (Julian Alps, Italy), *Surv. Geophys.*, 36, 231–252, 2015.~~

771 Dall'Asta, E., Delaloye, R., Diotri, F., Forlani, G., Fornari, M., Morra di Cella, U.,  
772 Pogliotti, P., Roncella, R., Santise, M.: Use of UAS in a high mountain landscape: the

773 case of gran sommetta rock glacier (AO), The International Archives of the  
774 Photogrammetry, Remote Sensing and Spatial Information Sciences, Volume XL-  
775 3/W3, 391–397, 2015a.

776 ~~Dall'Asta, E., Thoeni, K., Santise, M., Forlani, G., Giacomini, A., and Roncella, R.:~~  
777 ~~Network design and quality checks in automatic orientation of close-range~~  
778 ~~photogrammetric blocks, Sensors, 15, 7985–8008, 2015b.~~

779 Debella-Gilo, M. and Käab, A.: Sub-pixel precision image matching for measuring  
780 surface displacements on mass movements using normalized cross-correlation.  
781 Remote Sens. Environ., 115, 130–142, 2011.

782 ~~Deems, J. S., Painter, T. H., and Finnegan, D. C.: Lidar measurement of snow depth:~~  
783 ~~a review, J. Glaciol., 59, 467–479, 2013.~~

784 Favalli, M., Fornaciai, A., Isola, I., Tarquini, S., and Nannipieri, L.: Multiview 3D  
785 reconstruction in geosciences, Comput. Geosci., 44, 168–176, 2012.

786 ~~Fischer, L., Eisenbeiss, H., Käab, A., Huggel, C., and Haeberli, W.: Monitoring~~  
787 ~~topographic changes in a periglacial high-mountain face using high-resolution DTMs,~~  
788 ~~Monte Rosa East Face, Italian Alps, Permafrost Periglac., 22, 140–152, 2011.~~

789 Gauthier, D., Conlan, M., and Jamieson, B.: Photogrammetry of fracture lines and  
790 avalanche terrain: potential applications to research and hazard mitigation projects,  
791 Proceedings, International Snow Science Workshop, Banff, 29 September–3 October  
792 2014, 109–115, 2014.

793 ~~Geist, T. and Stotter, J.: Documentation of glacier surface elevation change with multi~~  
794 ~~temporal airborne laser scanner data — case study: Hintereisferner and~~  
795 ~~Kesselwandferner, Tyrol, Austria, Zeitschrift für Gletscherkunde und Glazialgeologie,~~  
796 ~~41, 77–106, 2007.~~

797 Glira, P., Pfeifer, N., Briese, C., Ressel, C.: A correspondence framework for ALS strip  
798 adjustments based on variants of the ICP algorithm, Photogramm. Fernerkun., 4,  
799 275–289, doi:10.1127/pfg/2015/0270, 2015.

800 Gómez-Gutiérrez, Á., de Sanjosé-Blasco, J. J., de Matías-Bejarano, J., and  
801 Berenguer-Sempere, F.: Comparing two photo-reconstruction methods to produce



802 high density point clouds and DEMs in the Corral del Veleta Rock Glacier (Sierra  
803 Nevada, Spain), *Remote Sensing*, 6, 5407–5427, 2014.

804 Gómez-Gutiérrez, Á., de Sanjosé-Blasco, J. J., Lozano-Parra, J., Berenguer-  
805 Sempere, F., and de Matías-Bejarano, J.: Does HDR pre-processing improve the  
806 accuracy of 3D models obtained by means of two conventional SfM-MVS software  
807 packages? The case of the Corral del Veleta Rock Glacier, *Remote Sensing*, 7,  
808 10269–10294, 2015.

809 Hartley, R. and Zisserman, A.: *Multiple View Geometry In Computer Vision*,  
810 Cambridge University Press, Cambridge, UK, 2003.

811 Haeberli, W.: Creep of mountain permafrost: internal structure and flow of alpine rock  
812 glaciers, *Mitteilungen der Versuchsanstalt für Wasserbau, Hydrologie und Glaziologie*  
813 *der ETH Zurich*, 77, 5–142, 1985.

814 ~~Haug, T., Rolstad, C., Elvehøy, H., Jackson, M., and Maalen-Johansen, I.: Geodetic~~  
815 ~~mass balance of the western Svartisen ice cap, Norway, in the periods 1968–1985~~  
816 ~~and 1985–2002, *Ann. Glaciol.*, 50, 119–125, 2009.~~

817 ~~Höfle, B., Geist, T., Rutzinger, M., and Pfeifer, N.: Glacier surface segmentation~~  
818 ~~using airborne laser scanning point cloud and intensity data, *International Archives of*~~  
819 ~~Photogrammetry, Remote Sensing and Spatial Information Sciences~~, 36, W52, 195–  
820 200, 2007.

821 ~~Höfle, B., and Rutzinger, M.: Topographic airborne LiDAR in geomorphology: A~~  
822 ~~technological perspective. *Zeitschrift für Geomorphologie, Supplementary Issues*,~~  
823 ~~55(2), 1–29, 2011.~~

824 Hosseiniveh, A., Sargeant, B., Erfani, T., Robson, S., Shortis, M., Hess, M., and  
825 Boehm, J.: Towards fully automatic reliable 3D acquisition: from designing imaging  
826 network to a complete and accurate point cloud, *Robotics and Autonomous Systems*,  
827 62, 1197–1207, 2014.

828 Huss, M.: Density assumptions for converting geodetic glacier volume change to  
829 mass change, *The Cryosphere*, 7, 877–887, doi:10.5194/tc-7-877-2013, 2013.

830 Immerzeel, W. W., Kraaijenbrink, P. D. A., Shea, J. M., Shrestha, A. B., Pellicciotti,  
831 F., Bierkens, M. F. P., and De Jong, S. M.: High-resolution monitoring of Himalayan

832 glacier dynamics using unmanned aerial vehicles, *Remote Sens. Environ.*, 150, 93–  
833 103, 2014.

834 ~~Isaksen, K., Ødegård, R. S., Eiken, T., and Sollid, J. L.: Composition, flow and~~  
835 ~~development of two tongue-shaped rock glaciers in the permafrost of Svalbard.~~  
836 ~~Permafrost and Periglacial Processes, 11, 241-257, 2000.~~

837 James, M. R. and Robson, S.: Straightforward reconstruction of 3D surfaces and  
838 topography with a camera: accuracy and geoscience application, *J. Geophys. Res.-*  
839 *Earth*, 117, F03017, doi:10.1029/2011JF002289, 2012.

840 James, M. R. and Robson, S.: Mitigating systematic error in topographic models  
841 derived from UAV and ground-based image networks, *Earth Surf. Proc. Land.* 39,  
842 1413–1420, doi:10.1002/esp.3609, 2014.

843 ~~Joerg, P. C. and Zemp, M.: Evaluating Volumetric Glacier Change Methods Using~~  
844 ~~Airborne Laser Scanning Data. *Geografiska Annaler: Series A, Physical Geography,*~~  
845 ~~96, 135–145, 2014.~~

846 Kääh, A.: Monitoring high-mountain terrain deformation from repeated air-and  
847 spaceborne optical data: examples using digital aerial imagery and ASTER data.  
848 *ISPRS Journal of Photogrammetry and remote sensing*, 57, 39–52, 2002.

849 Kääh, A.: Remote Sensing of Mountain Glaciers and Permafrost Creep. *Research*  
850 *Perspectives from Earth Observation Technologies and Geoinformatics,*  
851 *Schriftenreihe Physische Geographie, Glaziologie und Geomorphodynamik*, 48,  
852 University of Zurich, Zurich, Switzerland, 2005.

853 ~~Kääh, A. and Funk, M.: Modelling mass balance using photogrammetric and~~  
854 ~~geophysical data: a pilot study at Griesgletscher, Swiss Alps. *J. Glaciol.* 45, 575–583,~~  
855 ~~1999.~~

856 ~~Kääh, A., Haeberli, W., and Gudmundsson, G. H.: Analyzing the creep of mountain~~  
857 ~~permafrost using high precision aerial photogrammetry: 25 years of monitoring~~  
858 ~~Gruben rock glacier, Swiss Alps, *Permafrost Periglac.*, 8, 409–426, 1997.~~

859 Kääh, A., Kaufmann, V., Ladstädter, R., and Eiken, T.: Rock glacier dynamics:  
860 implications from high-resolution measurements of surface velocity fields, in: *Eighth*

861 International Conference on Permafrost, 21–25 July 2003, Zurich, Switzerland, Vol.  
862 1, 501–506, 2003.

863 Kääh, A., Girod, L., and Berthling, I.: Surface kinematics of periglacial sorted circles  
864 using structure-from-motion technology, *The Cryosphere*, 8, 1041–1056,  
865 doi:10.5194/tc-8-1041-2014, 2014.

866 ~~Kaufmann, V.: Deformation analysis of the Doesen rock glacier (Austria), in:  
867 *Proceedings of the 7th International Permafrost Conference, 23–27 June 1998,*  
868 *Yellowknife, Canada, 551–556, 1998.*~~

869 ~~Kaufmann, V. and Ladstädter R.: Application of terrestrial photogrammetry for glacier  
870 monitoring in Alpine environments, *Proceedings of the 21st Congress of ISPRS,*  
871 *Beijing, China, 3–11 July 2008, Vol. 37, Part B8, 813–818, 2008.*~~

872 ~~Knoll, C. and Kerschner, H.: A glacier inventory for South Tyrol, Italy, based on  
873 airborne laserscanner data, *Ann. Glaciol.*, 50, 46–52, 2010.~~

874 ~~Kodde, M. P., Pfeifer, N., Gorte, B. G. H., Geist, T., and Höfle, B.: Automatic glacier  
875 surface analysis from airborne laser scanning, *International Archives of the*  
876 *Photogrammetry, Remote Sensing and Spatial Information Sciences*, 36, 221–226,  
877 2007.~~

878 ~~Maas, H. G., Schwalbe, E., Dietrich, R., Bässler, M., and Ewert, H.: Determination of  
879 spatiotemporal velocity fields on glaciers in West-Greenland by terrestrial image  
880 sequence analysis, *International Archives of Photogrammetry, Remote Sensing and*  
881 *Spatial Information Science*, 37, 1419–1424, 2008.~~

882 Micheletti, N., Chandler, J. H., and Lane, S. N.: Investigating the geomorphological  
883 potential of freely available and accessible Structure-from-Motion photogrammetry  
884 using a smartphone, *Earth Surf. Proc. Land.*, 40, 473–486, doi:10.1002/esp.3648,  
885 2014.

886 ~~Müller, J., Gärtner-Roer, I., Thee, P., and Ginzler, C.: Accuracy assessment of  
887 airborne photogrammetrically derived high-resolution digital elevation models in a  
888 high mountain environment. *ISPRS Journal of Photogrammetry and Remote*  
889 *Sensing*, 98, 58–69, 2014.~~

890 Nilosek, D., Sun, S., and Salvaggio, C.: Geo-accurate model extraction from three-  
891 dimensional image-derived point clouds, in: Proceedings of SPIE, Algorithms and  
892 Technologies for Multispectral, Hyperspectral, and Ultraspectral Imagery XVIII, 23  
893 April 2012, Baltimore, MD, USA, 8390, 83900J, doi:10.1117/12.919148, 2012.

894 Nocerino, E., Menna, F., and Remondino, F.: Accuracy of typical photogrammetric  
895 networks in cultural heritage 3D modeling projects, ISPRS-International Archives of  
896 the Photogrammetry, Remote Sensing and Spatial Information Sciences, 1, 465–472,  
897 2014.

898 ~~Pellikka, P. and Rees, W. G.: Remote Sensing Of Glaciers: Techniques For  
899 Topographic, Spatial and Thematic Mapping of Glaciers, CRC Press, University of  
900 Cambridge, Cambridge, UK, 2009.~~

901 Piermattei, L., Carturan, L., and Guarnieri, A.: Use of terrestrial photogrammetry  
902 based on structure from motion for mass balance estimation of a small glacier in the  
903 Italian Alps, Earth Surf. Proc. Land., 40, 1791–1802, doi:10.1002/esp.3756, 2015.

904 ~~Prosdocimi, M., Sofia, G., Dalla Fontana, G., Tarolli, P.: Bank erosion in agricultural  
905 drainage networks: effectiveness of Structure-from-Motion for post-event analysis,  
906 Earth Surf. Proc. Land., 40, 1891–1906, doi:10.1002/esp.3767, 2015.~~

907 Ryan, J. C., Hubbard, A. L., Box, J. E., Todd, J., Christoffersen, P., Carr, J. R., Holt,  
908 T. O., and Snooke, N.: UAV photogrammetry and structure from motion to assess  
909 calving dynamics at Store Glacier, a large outlet draining the Greenland ice sheet,  
910 The Cryosphere, 9, 1–11, doi:10.5194/tc-9-1-2015, 2015.

911 Roer, I. and Nyenhuis, M.: Rockglacier activity studies on a regional scale:  
912 comparison of geomorphological mapping and photogrammetric monitoring, Earth  
913 Surf. Proc. Land., 32, 1747–1758, 2007.

914 Seppi, R., Carton, A., Zumiani, M., Dall’Amico, M., Zampedri, G., and Rigon, R.:  
915 Inventory, distribution and topographic features of rock glaciers in the southern region  
916 of the Eastern Italian Alps (Trentino). Geografia Fisica e Dinamica Quaternaria 35,  
917 185–197, doi:10.4461/GFDQ.2012.35.17, 2012.

918 ~~Shenk, T.: Digital Photogrammetry Vol. 1, Terra Science, Laurelville, OH, USA, 1,  
919 43135, 428 pp., 1999.~~

920 Solbø, S. and Storvold, R.: Mapping svalbard glaciers with the cryowing uas, ISPRS  
921 International Archives of the Photogrammetry, Remote Sensing and Spatial  
922 Information Sciences, XL-1/W2, 373–377, 2013.

923 ~~Stumpf, A., Malet, J. P., Allemand, P., Pierrot-Deseilligny, M., and Skupinski, G.:  
924 Ground-based multi-view photogrammetry for the monitoring of landslide deformation  
925 and erosion, *Geomorphology*, 231, 130–145, 2015.~~

926 ~~Tarolli, P.: High-resolution topography for understanding Earth surface processes:  
927 opportunities and challenges, *Geomorphology*, 216, 295–312, 2014.~~

928 Tonkin, T. N., Midgley, N. G., Graham, D. J., and Labadz, J. C.: The potential of  
929 small unmanned aircraft systems and structure-from-motion for topographic surveys:  
930 a test of emerging integrated approaches at Cwm Idwal, North Wales,  
931 *Geomorphology*, 226, 35–43, 2014.

932 Tseng, C.-M., Lin, C. W., Dalla Fontana, G., Tarolli, P.: The topographic signature of  
933 a Major Typhoon, *Earth Surf. Proc. Land.*, 40, 1129–1136, 2015.

934 Verhoeven, G., Karel, W., 'tuhec, S., Doneus, M., Trinks, I., and Pfeifer, N.: Mind your  
935 grey tones – examining the influence of decolourization methods on interest point  
936 extraction and matching for architectural image-based modelling, in: 3D-Arch 2015–  
937 3D Virtual Reconstruction and Visualization of Complex Architectures (ISPRS WG  
938 V/4, CIPA), 25–27 February 2015, Vol. 40, ISPRS, Avila, Spain, 307–314, 2015.

939 Wackrow, R. and Chandler, J.: Minimising systematic error surfaces in digital  
940 elevation models using oblique convergent imagery, *Photogramm. Rec.*, 26, 16–31,  
941 2011.

942 ~~Welch, R., and Howarth, P. J.: Photogrammetric measurements of glacial landforms,  
943 *Photogramm. Rec.*, 6, 75–96, doi:10.1111/j.1477-9730.1968.tb00915.x, 1968.~~

944 Wenzel, K., Rothermel, M., Fritsch, D., and Haala, N.: Image acquisition and model  
945 selection for multi-view stereo, *Int. Arch. Photogramm. Remote Sens. Spatial Inf. Sci.*,  
946 251–258, 2013.

947 Whitehead, K., Moorman, B. J., and Hugenholtz, C. H.: Brief Communication: Low-  
948 cost, ondemand aerial photogrammetry for glaciological measurement, *The  
949 Cryosphere*, 7, 1879–1884, doi:10.5194/tc-7-1879-2013, 2013.

950 ~~Whitehead, K., Moorman, B., and Wainstein, P.: Instruments and Methods Measuring~~  
951 ~~daily surface elevation and velocity variations across a polythermal arctic glacier~~  
952 ~~using ground based photogrammetry, J. Glaciol., 60, 1208–1220,~~  
953 ~~doi:10.3189/2014JoG14J080, 2014.~~

954 Zemp, M., Thibert, E., Huss, M., Stumm, D., Denby, C. R., Nuth, C., Nussbaumer, S.  
955 U., Moholdt, G., Mercer, A., Mayer, C., Joerg, P. C., Jansson, P., Hynek, B., Fischer,  
956 A., Escher-Vetter, H., Elvehøy, H., and Andreassen, L. M.: Reanalysing glacier mass  
957 balance measurement series. The Cryosphere, 7, 1227-1245, doi:10.5194/tc-7-1227-  
958 2013, 2013.

959

960

961

962

963

964

965

966

967

968

969

970

971

972

973

974

975 **Table 1.** Date and main parameters of available LiDAR data.

Date	Aircraft	Laser scanner model	Laser scanner rate	Max. scan angle	Scan frequency	Point density [pts·m <sup>-2</sup> ]
24 Sept. 2014	Elicopter AS350 B3	Optech ALTM GEMINI (04SEN164)	100 kHz	46°	34 Hz	5.1
22 Sept. 2013	Cessna 404 D-IDOS	ALTM 3100	70,000 Hz	±25°	32 Hz	0.9
17 Sept. 2003	—	—	—	—	—	0.5

976

977 **Table 2.** Data acquisition settings and processing results of the photogrammetric  
 978 surveys for both case studies. The GCPs error is the average transformation  
 979 residuals error [m] and root mean square reprojection error for the GCPs [pix] during  
 980 the bundle adjustment computation. The image quality represents the downsized of  
 981 the images resolution during the dense matching computation. “Ultra high” means full  
 982 resolution, “High” a downsized of 50% before the image matching processing. The  
 983 ground sample distance (GSD) is the average pixel size on the ground. The standard  
 984 deviation of ICP registration is reported in the table.

	La Mare glacier		Rock glacier
	4 September 2013	27 September 2014	27 September 2014
<i>Input data</i>			
Camera type	Nikon 600D		Canon 5D Mark III
Focal Length	25 mm		28 mm
Image size	5184 x 3456 pix	5184 x 3456 pix	5760 x 3840 pix
N° Images	37		198
<i>Processing data</i>			
Reprojection error	0.43 pix (1.76 max)	0.40 pix (3.75 max)	0.38 pix (1.20 max)
GCPs error	1.52 m 1.48 pix	1.14 m 1.96 pix	0.62 m 1.86 pix
Image quality	Ultra high		High
Mean GSD	0.16 m/pix		0.064 m/pix
Dense point cloud	49,844,094 pts	55,114,074 pts	56,171,705 pts
Point density	37 pts m <sup>-2</sup>	20 pts m <sup>-2</sup>	244 pts m <sup>-2</sup>
<i>Post-processing data</i>			
Filtered point cloud /subsampled	15,617,342 pts (sampled 0.20 m)	24,226,221 pts (sampled 0.20 m)	4,517,143 pts (sampled 0.10 m)
Point density	8 pts m <sup>-2</sup>	9 pts m <sup>-2</sup>	21 pts m <sup>-2</sup>
ICP transformation	0.14 m	0.15 m	0.10 m

985

986

987

988

989 **Table 3.** Results of comparisons between SfM-MVS-based DEMs vs. ALS-based  
 990 DEMs in the common area and for the bare-ground stable area and glacier.

<b>Elevation differences [m] cell size 1 m x 1m</b>									
DEMs	Common SfM-MVS bare-ground area				Common SfM-MVS glacier area				
	<i>Min</i>	<i>Max</i>	<i>Mean</i>	$\sigma$	<i>Min</i>	<i>Max</i>	<i>Mean</i>	$\sigma$	
SfM-MVS - ALS 2013 2013	-19.59	33.61	-0.42	1.72	-9.91	12.04	-0.13	0.78	
SfM-MVS - ALS 2014 2014	-18.48	22.42	0.03	0.74	-18.17	11.41	0.23	0.65	
SfM-MVS - SfM-MVS 2014 2013	-33.12	14.19	0.38	1.73	-12.44	12.33	1.58	1.42	
ALS 2014 - ALS 2013	-15.38	10.81	-0.09	0.29	-14.61	7.37	1.30	0.97	

991

992 **Table 4.** Mass balance calculations on La Mare Glaciers using different combinations  
 993 of SfM-MVS and ALS DEMs.

<b>Mass balance estimation</b>									
DEMs cell size 10 m	Spatial coverage [m <sup>2</sup> ]	Average elevation		Volume change		Mass balance			
		changes [m]		[m <sup>3</sup> ]		[m w.e]			
		<i>Raw</i>	<i>Corrected</i>	<i>Raw</i>	<i>Corrected</i>	<i>Raw</i>	<i>Corrected</i>		
SfM-MVS - SfM-MVS 2014 2013	1,834,800	1.81	1.45	3,320,988	2,660,460	1.09	0.87		
ALS 2014 - ALS 2013	(~88%)	1.47	1.56	2,697,156	2,862,288	0.88	0.94		
SfM-MVS - ALS 2013 2014	1,938,700	1.64	1.70	3,179,468	3,295,790	0.98	1.02		
ALS 2014 - ALS 2013	(~93%)	1.41	1.50	2,733,567	2,908,050	0.85	0.90		
ALS 2014 - ALS 2013	2,072,700 (entire glacier)	1.43	1.52	2,963,961	3,150,504	0.86	0.91		

994

995

996

997

998

999

1000

1001

1002

1003



1004 **Table 5.** Statistics of elevation changes in the rock glacier and in bed-bare ground  
 1005 stable area a off rock glacier from September 2014 to September 2013 and September  
 1006 2003 in the ALS reconstructed area and in the common ALS and SfM-MVS coverage  
 1007 area.

Data		Elevation changes [m]							
		ALS Reconstructed area				SfM-MVS Reconstructed area			
		Stable area		Rock glacier		Stable area		Rock glacier	
		Mean	$\sigma$	Mean	$\sigma$	Mean	$\sigma$	Mean	$\sigma$
SfM-MVS 2014	- ALS 2014	—	—	—	—	0.05	0.31	0.02	0.17
SfM-MVS 2014	- ALS 2013	—	—	—	—	0.01	0.33	-0.04	0.18
ALS 2014	- ALS 2013	-0.05	0.19	-0.07	0.12	-0.05	0.20	-0.07	0.12
SfM-MVS 2014	- ALS 2003	—	—	—	—	0.06	0.33	-0.16	0.49
ALS 2014	- ALS 2003	-0.01	0.22	-0.18	0.46	-0.00	0.21	-0.18	0.47
ALS 2013	- ALS 2003	0.04	0.21	-0.11	0.41	—	—	—	—

1008

1009 **Table 6.** Velocity statistics in three distinct areas of the rock glacier and in stable area  
 1010 outside the rock glacier evaluated comparing the 2003 and 2014 ALS DEMs and the  
 1011 photogrammetric DEM for the 2014 survey epoch.

		Horizontal movements between 2003 and 2014 [cm yr <sup>-1</sup> ]									
		ALS 2003 - ALS 2014					ALS 2003 - SfM-MVS 2014				
		No. points	Min	Max	Mean	$\sigma$	No. points	Min	Max	Mean	$\sigma$
Area 1	41	7.3	43.3	26.8	8.9	36	6.8	47.5	26.3	10.3	
Area 2	13	4.4	27.4	18.9	7.0	11	9.0	27.9	18.1	6.4	
Area 3	26	4.5	16.5	9.4	4.0	24	4.5	18.2	9.0	4.1	
Off rock glacier	65	0.0	10.7	3.6	3.1	23	0.0	13.6	5.3	4.2	

1012

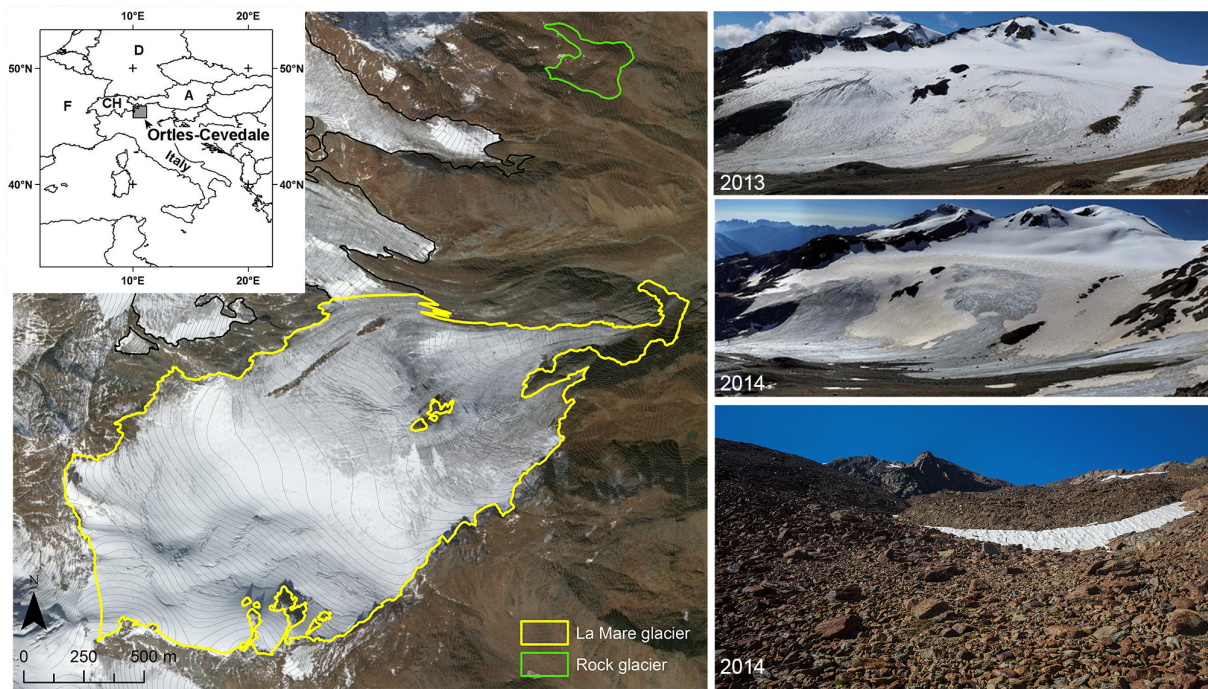
1013

1014

1015

1016

1017



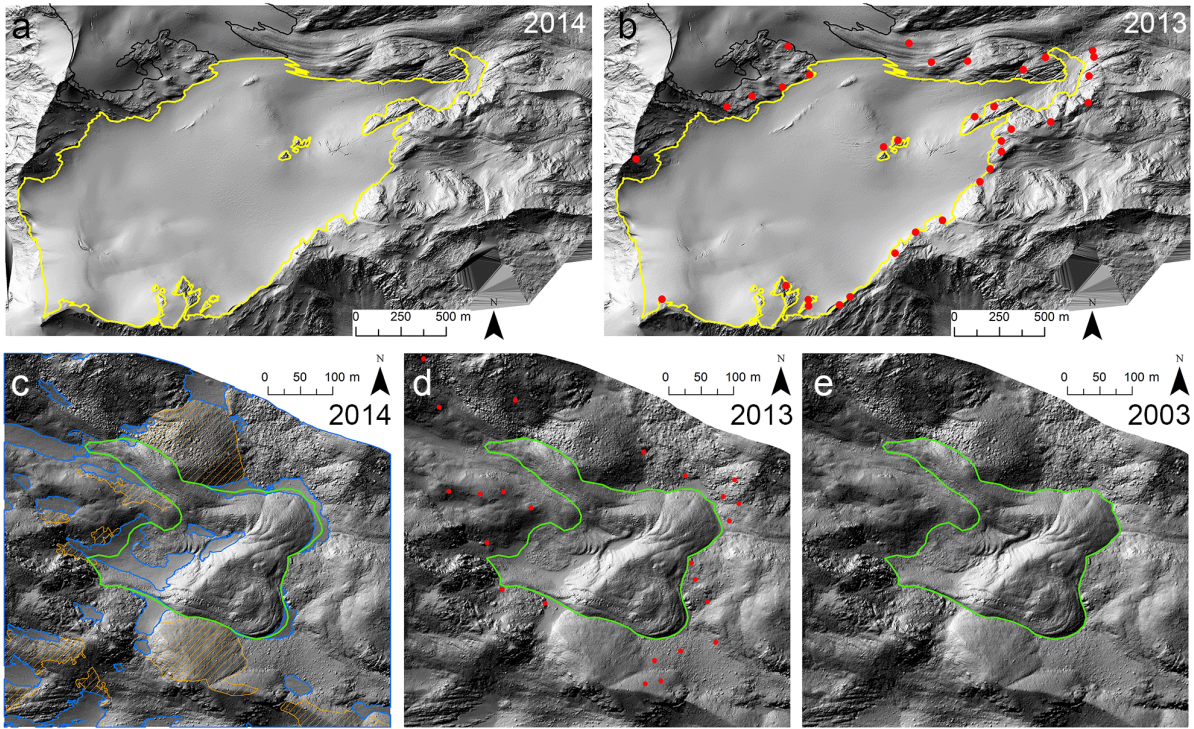
1018

1019 **Figure 1.** Geographic setting of study areas. Panorama view of the La Mare Glacier  
 1020 from the same camera position on 4 September 2013 and 27 September 2014. The  
 1021 lower right photograph shows the front of the meridional lobe of the AVDM3 Rock  
 1022 Glacier, which was surveyed on 27 September 2014.

1023

1024

1025

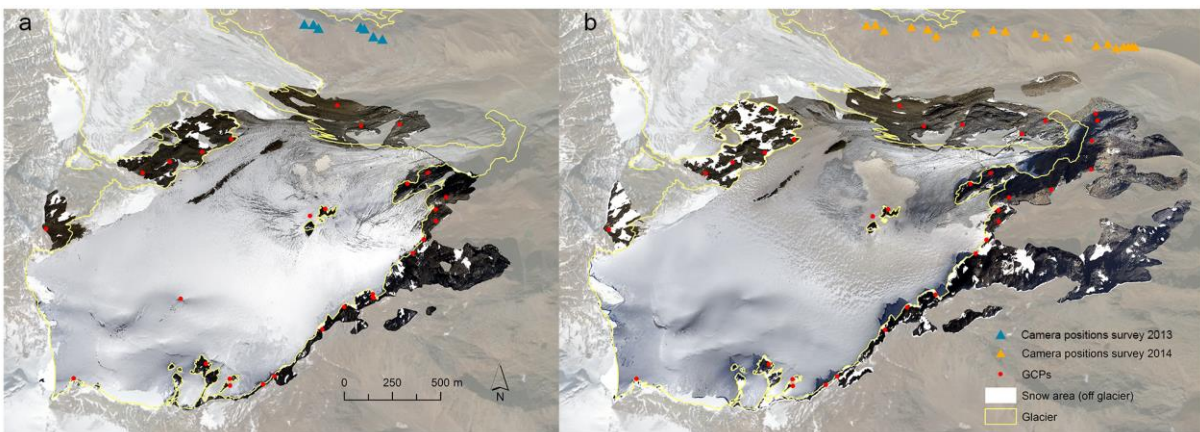


1026

1027 **Figure 2.** ALS shade DEMs of la Mare glacier acquired on **(a)** September 24, 2014  
 1028 and **(b)** September 21, 2013. The ALS DEMs of rock glacier acquired on **(c)** 2014,  
 1029 **(d)** 2013 and **(e)** 2003. The red dots represent the selected GCPs in 2013 DEM used  
 1030 in the photogrammetric approach. The snow accumulation areas and  
 1031 geomorphologically-active areas outside the rock glacier were excluded during the  
 1032 ICP computation between 2013 and 2003, 2014 ALS point cloud.

1033

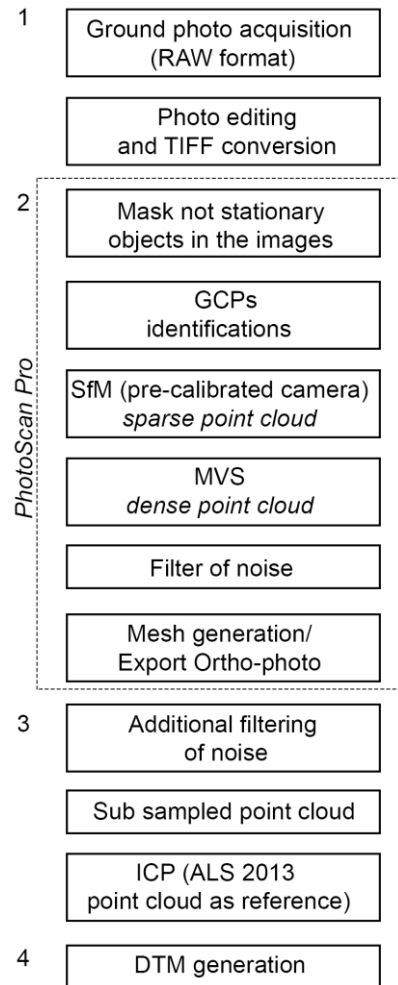
1034



1035

1036 **Figure 3.** Orthophoto-images of SfM-MVS 3D model of La Mare glacier surveyed on  
 1037 **(a)** 4 September 2013 and **(b)** 27 September 2014. The white areas in the ortho-  
 1038 images represent the snow-covered area in the rock stable area. The red dots  
 1039 outside the glacier area are the GCPs and the triangles identified the camera  
 1040 locations.

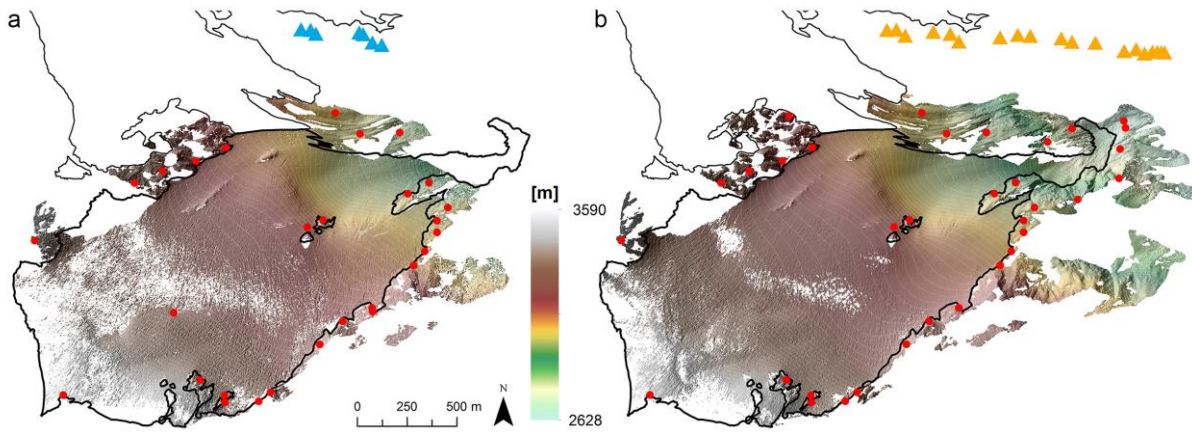
1041



1042

1043 **Figure 4.** Workflow illustrating the photo-based 3D reconstruction process used in  
 1044 this work for both case studies, starting from images collection to DEM generation.

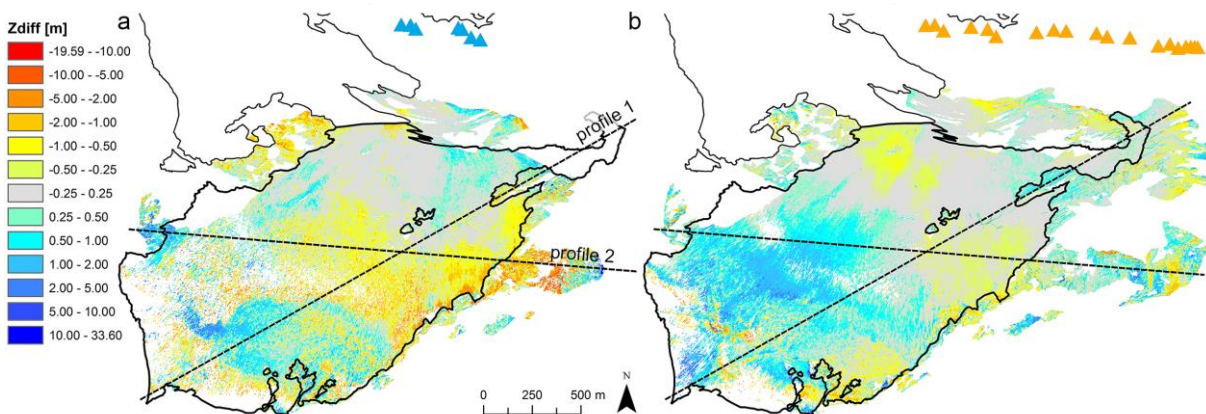
1045



1046  La Mare glacier    ● GCPs    ▲ Camera position survey 2013    ▲ Camera position survey 2014

1047 **Figure 5.** Hillshaded DEMs of La Mare glacier derived from photogrammetric  
 1048 measurements on **(a)** 4 September 2013 and **(b)** 27 September 2014.

1049

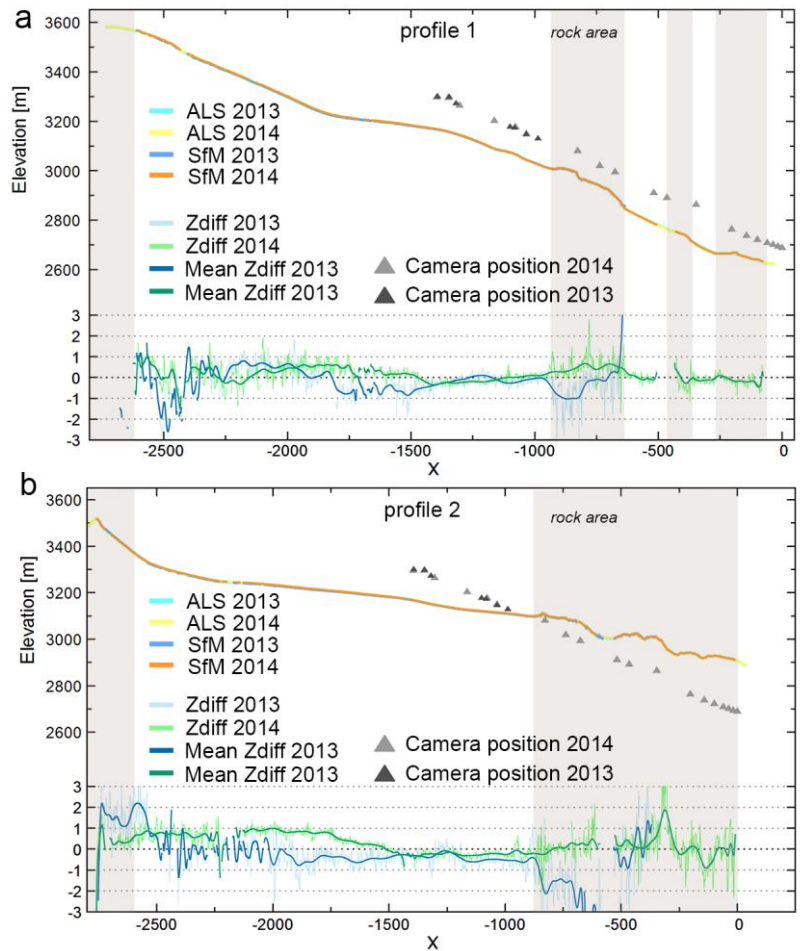


1050

1051 **Figure 6.** Spatial distribution of elevation differences between photogrammetric and  
 1052 ALS-based DEMs on **(a)** 2013 and **(b)** 2014.

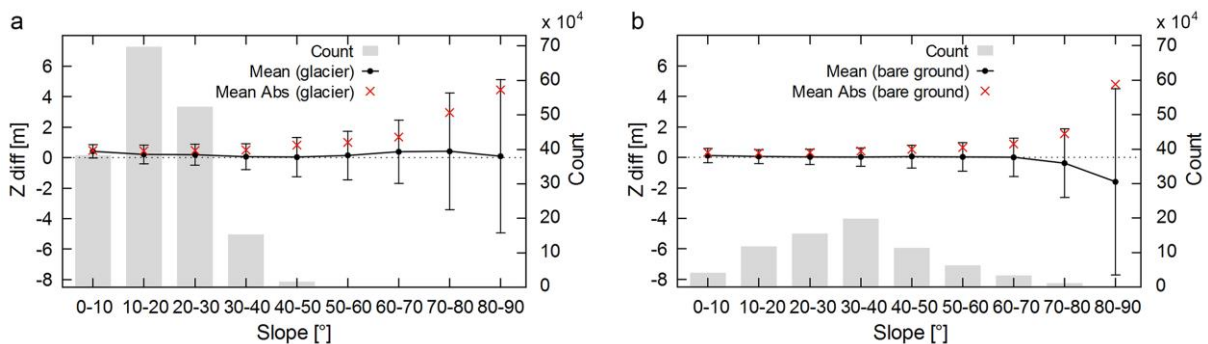
1053

1054



1055

1056 **Figure 7.** Cross sections through the La Mare glacier DEMs show the glacier  
 1057 elevation change and the difference between 2013 and 2014 in SfM-MVS and ALS-  
 1058 based DEMs. The location of **(a)** the profile 1 and **(b)** profile 2 is indicated in Fig. 6.  
 1059 The x-axis zero has been fixed at the first camera position of the 2014 survey and the  
 1060 minimum and maximum values of the z-difference set to  $\pm 3$  m.

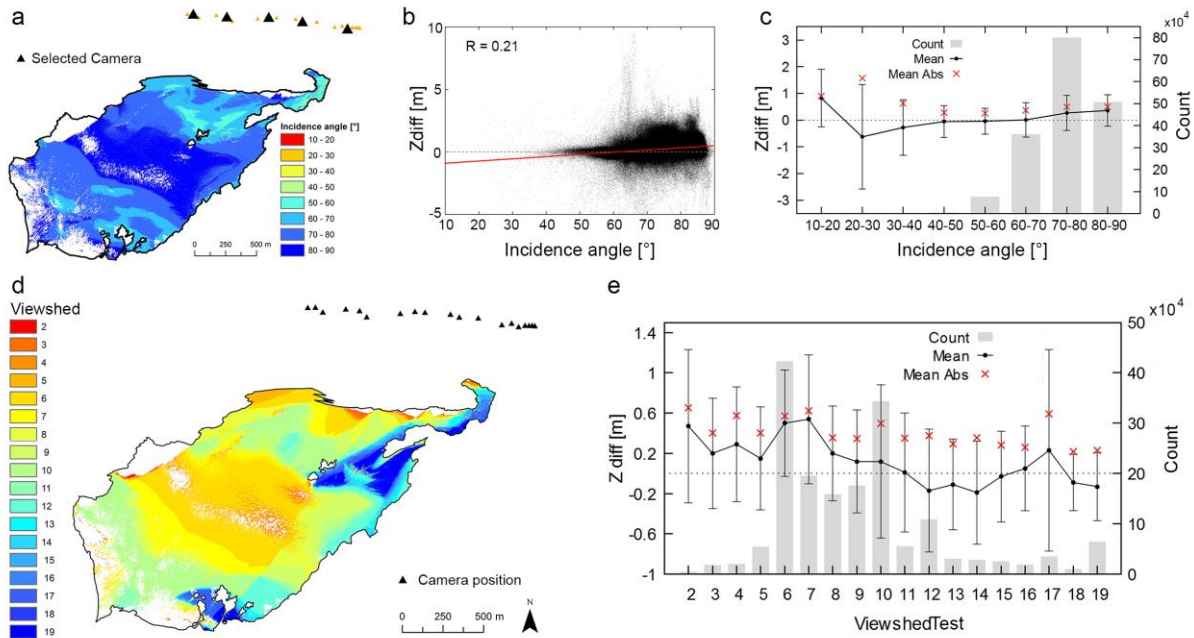


1061

1062 **Figure 8.** Mean, mean of the absolute values and standard deviation of the 2014  
 1063 DoD between SfM-MVS and ALS-based DEM depending on slope calculated **(a)** in

1064 the glacier area and **(b)** in the bare ground outside glacier covered by rock. The grey  
 1065 bars show the count of cells at any given slope (y-axis on the right).

1066

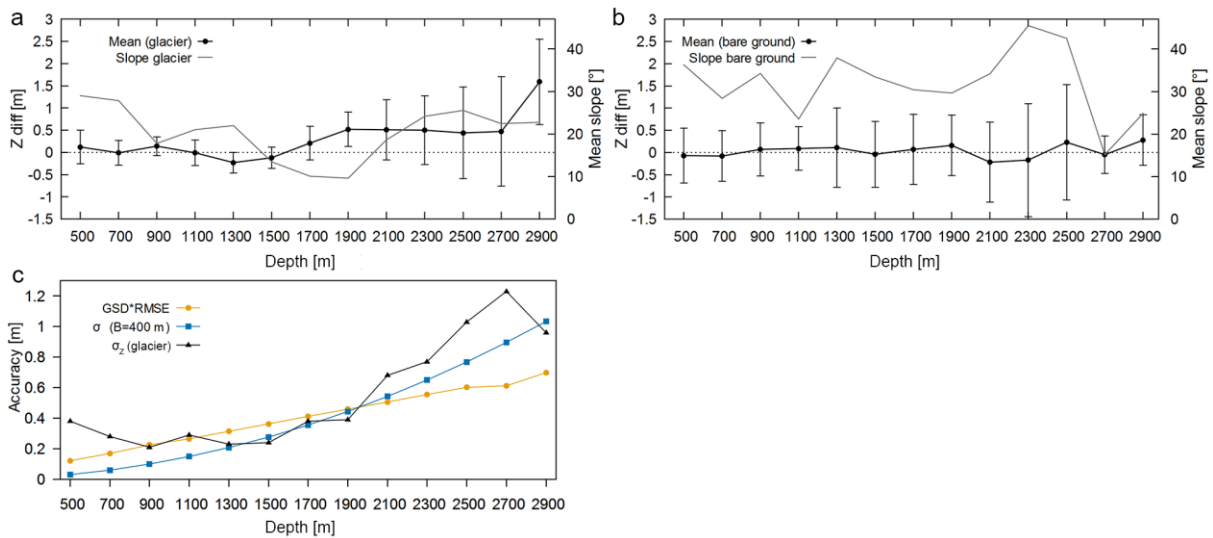


1067

1068 **Figure 9.** Mean incidence angles between five cameras positions and vectors normal  
 1069 to the surface and viewshed analysis. (a) Map of the mean incidence angle  
 1070 calculated for five representative camera positions; (b) the scatterplot of the elevation  
 1071 difference and the mean incidence angle for the five camera positions; (c) mean with  
 1072 one standard deviation y bars and mean of the absolute value of elevation  
 1073 differences for the mean incidence angle intervals calculated for 5 selected camera;  
 1074 (d) map of the viewshed reconstructed area visible from all camera; (e) mean with  
 1075 one standard deviation y bars and mean of the absolute value of elevation  
 1076 differences for the viewshed reconstructed area.~~Mean incidence angles between five~~  
 1077 ~~cameras positions and vectors normal to the surface. (a) Map of the mean incidence~~  
 1078 ~~angle calculated for five representative camera positions; (b) the scatterplot of the~~  
 1079 ~~elevation difference and the mean incidence angle for the five camera positions; (c)~~  
 1080 ~~mean with one standard deviation y bars and mean of the absolute value of elevation~~  
 1081 ~~differences for the mean incidence angle intervals calculated for 5 selected camera;~~  
 1082 ~~(d) map of the viewshed reconstructed area visible from all camera; (e) mean with~~  
 1083 ~~one standard deviation y bars and mean of the absolute value of elevation~~  
 1084 ~~differences for the viewshed reconstructed area.~~

1085 Frequency distribution histograms of incidence angles calculated for the  
 1086 corresponding surface and (b) the scatterplot of the elevation difference and  
 1087 incidence angle for the five camera positions; (c) mean of elevation differences with  
 1088 one standard deviation y bars calculated for each camera and for incidence angle  
 1089 intervals; (d) map of the locations of the selected cameras with the viewshed  
 1090 reconstructed area visible from each camera point.

1091

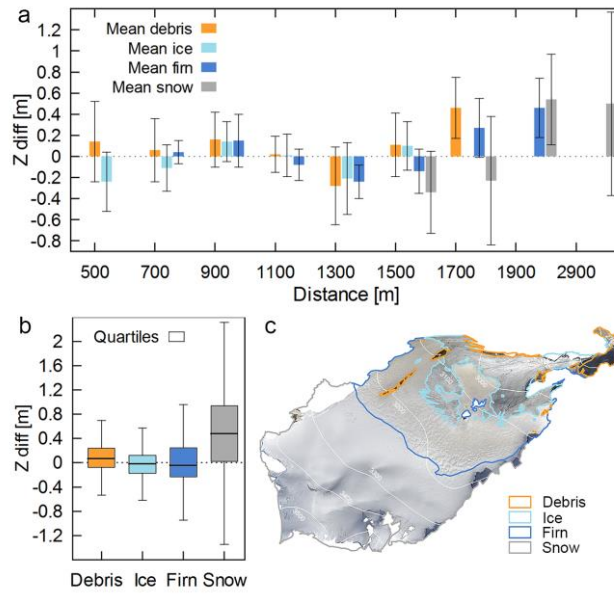


1092

1093 **Figure 10.** Mean and standard deviation of the 2014 DoD between SfM-MVS and  
 1094 ALS-based DEM depending on depth calculated (a) in the glacier area and (b) in the  
 1095 bare ground outside glacier covered by rock. The trend of the average slope angle  
 1096 for depth intervals is shown on the right y-axis. (c) Comparison of  $\sigma_z$  measured in the  
 1097 glacier reconstructed area, the theoretical depth accuracy estimated according to the  
 1098 Eq. (1) and the GSD multiplied for the GCPs RMSE for the depth intervals.

1099

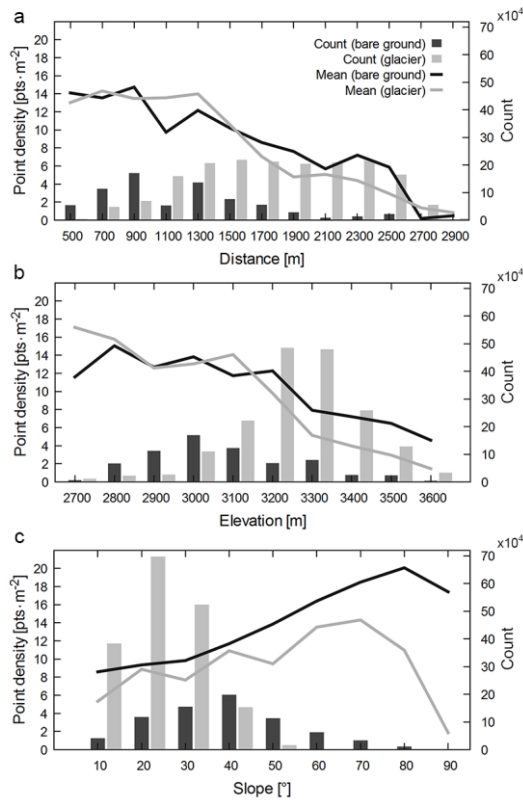




1100

1101 **Figure 11.** Elevation difference between the 2014 SfM-MVS and ALS-based DEMs  
 1102 calculated for different substrata. The figure shows **(a)** the mean and standard  
 1103 deviation of z-difference for four substrata (debris, ice, firn, and snow) grouped by  
 1104 distance from camera position; **(b)** the box plot of the z-difference for four substrata.  
 1105 In the box-whisker plot, values which exceed  $1.5 * IQR$  were considered outliers. In  
 1106 panel **(c)** the orthophoto of the glacier on 27 September 2014 and map of substrata.

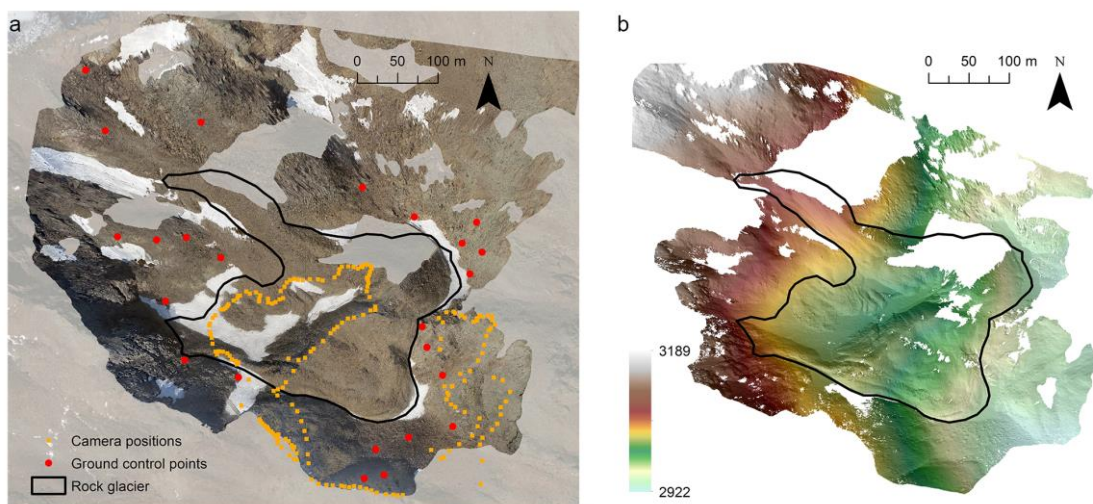
1107



1108

1109 **Figure 12.** Relationships between point density of the 2014 photogrammetric 3D  
 1110 model and **(a)** camera-object distance, **(b)** elevation and **(c)** slope calculated for the  
 1111 glacier and rock stable area outside glacier. The point density was estimated using  
 1112 the filtered and subsampled point cloud.

1113

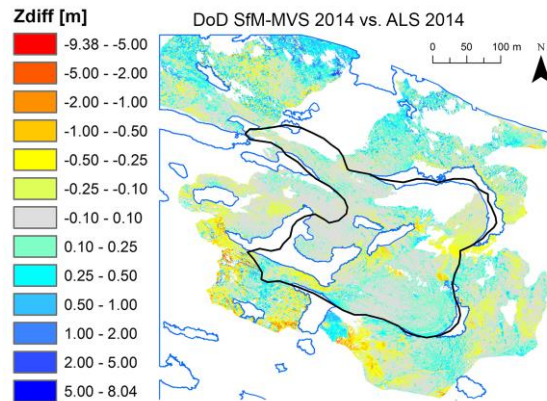


1114

1115 **Figure 13.** Correspondence between **(a)** the orthophoto of SfM-MVS 3D model of  
 1116 rock glacier surveyed on 27 September 2014 and **(b)** the hillshade model of rock

1117 glacier model calculated at the same data and hour of the images acquisition. The  
 1118 holes in the DEM represent not reconstructed area.

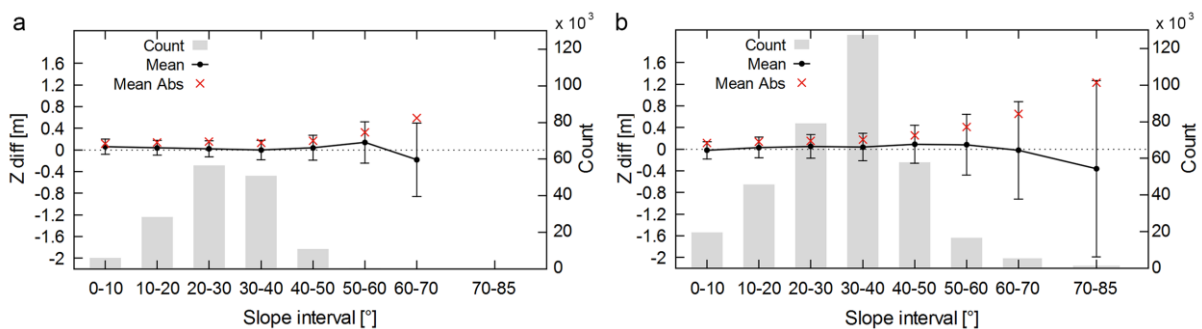
1119



1120

1121 **Figure 14.** Spatial distribution of elevation differences between photogrammetric and  
 1122 ALS-based DEM acquired on 27 September 2014 and 24 September 2014,  
 1123 respectively. The blue shape is the snow accumulation areas excluded during the  
 1124 DEMs comparison.

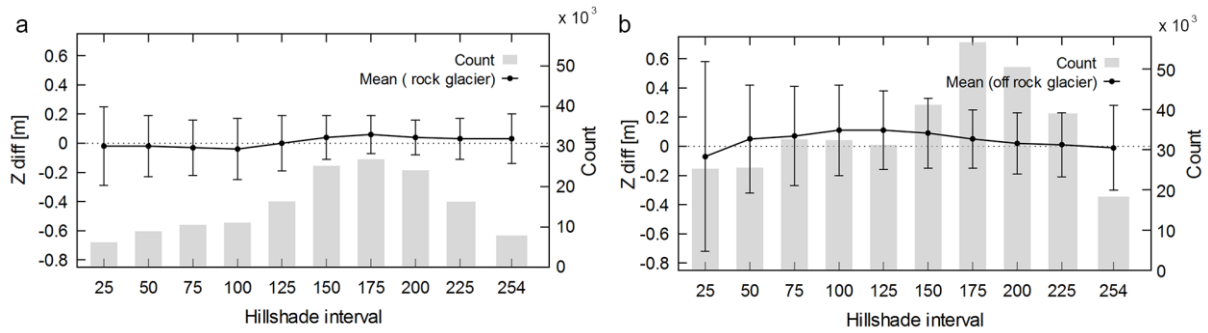
1125



1126

1127 **Figure 15.** Mean, mean of the absolute values and standard deviation of elevation  
 1128 differences between 2014 SfM-MVS and ALS-based DEMs calculated for the slope  
 1129 interval **(a)** in the rock glacier reconstructed area and **(b)** in the bare ground outside  
 1130 the rock glacier.

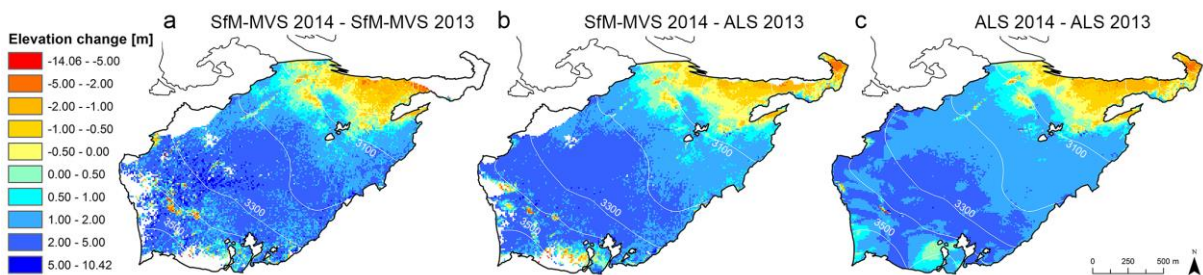
1131



1132

1133 **Figure 16.** Elevation differences between 2014 SfM-MVS and ALS-based DEMs  
 1134 calculated for the hillshade interval **(a)** in the rock glacier reconstructed area and **(b)**  
 1135 in the bare ground outside the rock glacier. Lowest values represent shadowed area  
 1136 whilst lighted areas present the highest values.

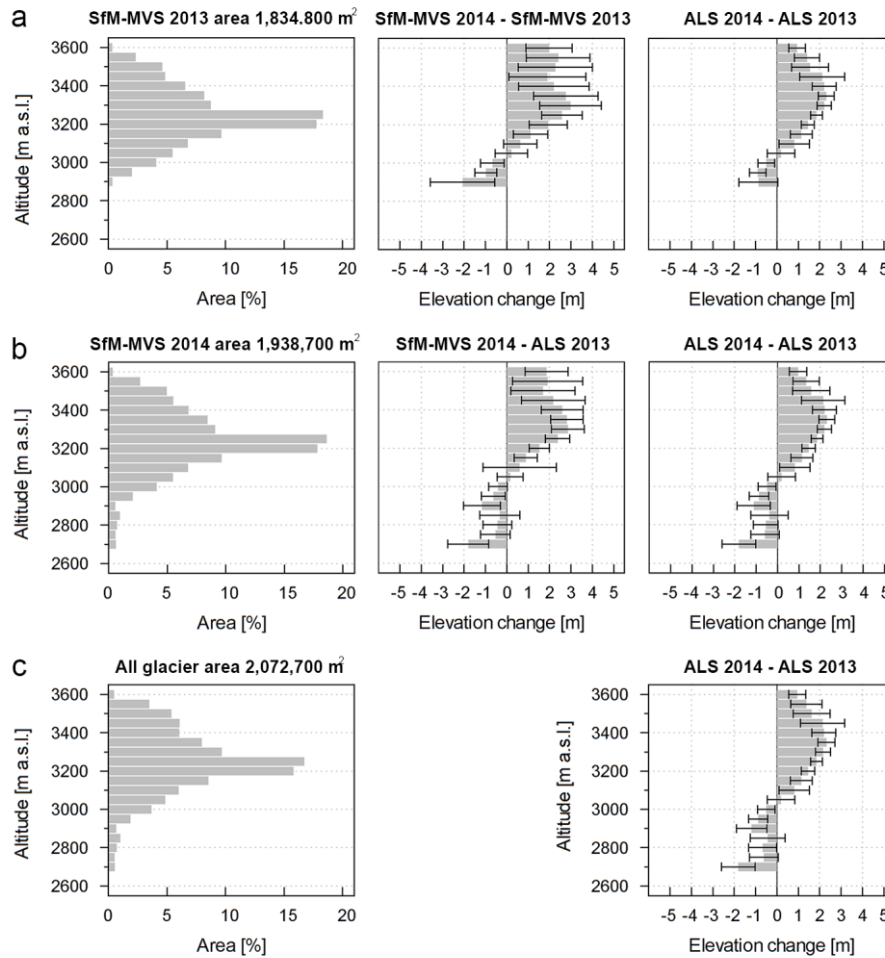
1137



1138

1139 **Figure 17.** Spatial distribution of elevation changes between **(a)** SfM-MVS 2014 and  
 1140 SfM-MVS 2013 DEMs **(b)** SfM-MVS 2014 and ALS 2013 over the area of the glacier  
 1141 with common coverage and **(c)** ALS 2014 and ALS 2013 over the entire glacier.

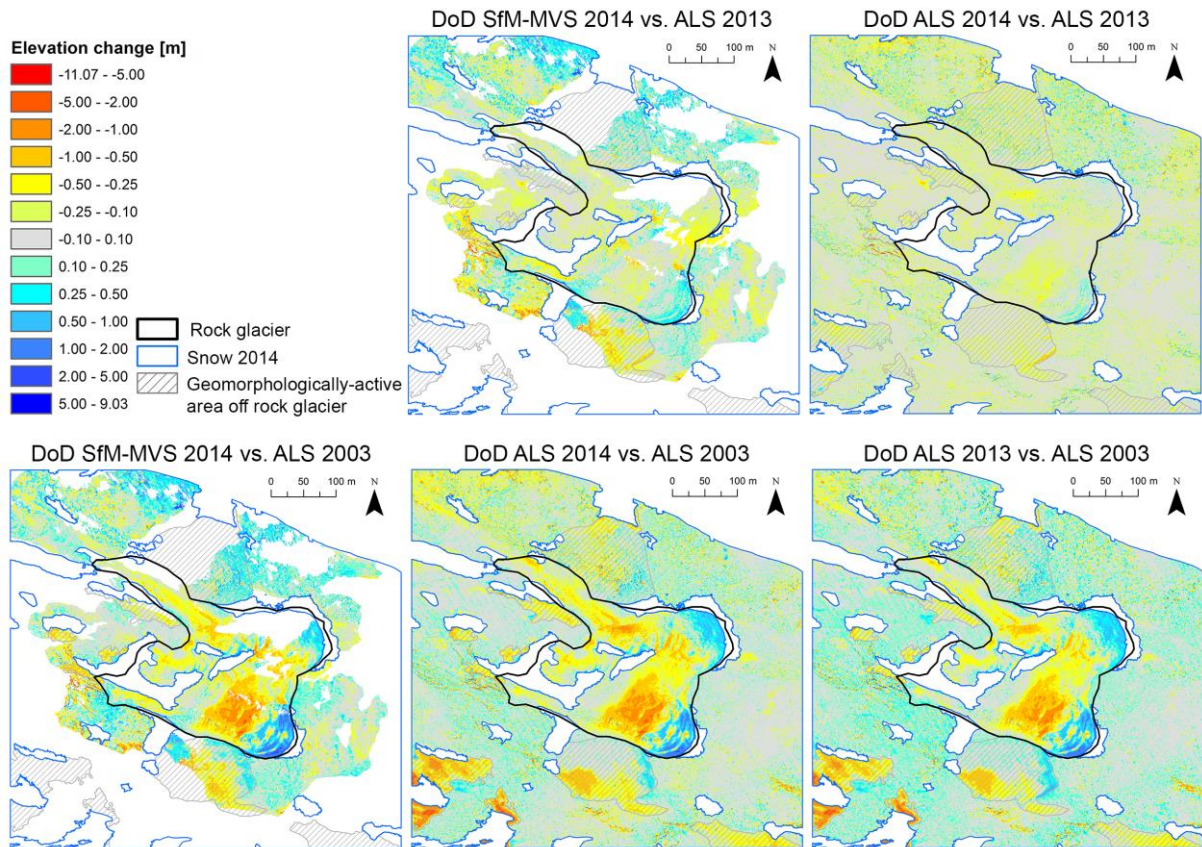
1142



1143

1144 **Figure 18.** Area-altitude distribution and surface elevation change with standard  
 1145 deviation for the glaciological year 2014/2013 displayed for altitudinal bands with 50  
 1146 m interval. The elevation change were calculated between **(a)** SfM-MVS DEMs of  
 1147 2013 and 2014 in the 2013 photogrammetric reconstructed area; **(b)** SfM-MVS DEMs  
 1148 of 2014 and ALS DEM of 2014 in the 2014 photogrammetric reconstructed area; **(c)**  
 1149 ALS DEMs of 2013 and 2014 of the entire glacier. The photogrammetric results were  
 1150 compared with the corresponding ALS result calculated in the same area.

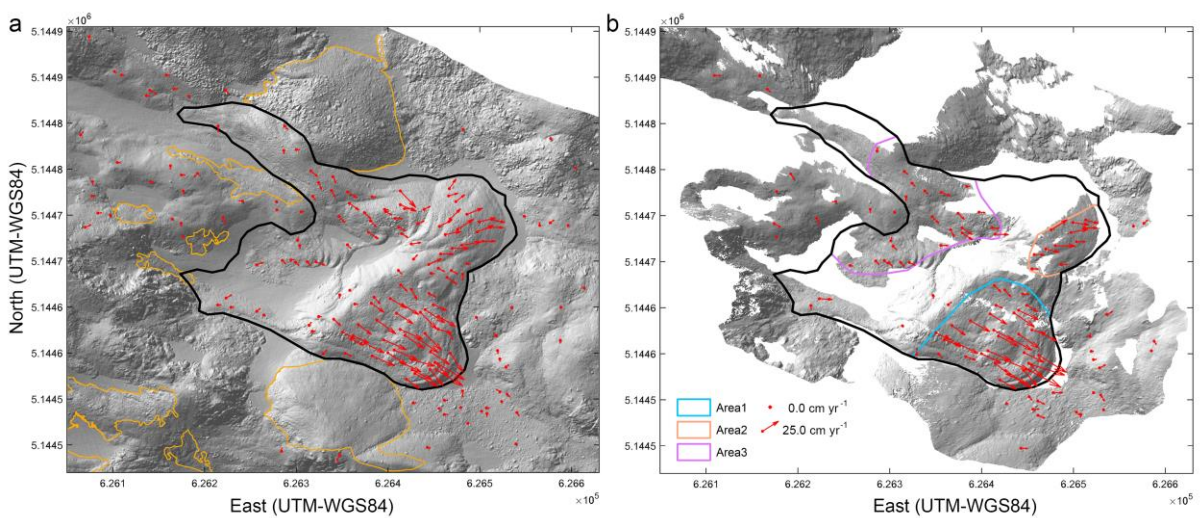
1151



1152

1153 **Figure 19.** Spatial distribution of elevation changes from September 2014 to  
 1154 September 2013 and September 2003 between the DEMs derived from SfM-MVS  
 1155 and ALS.

1156



1157

1158 **Figure 20.** Displacement vectors of the rock glacier between 2003 and 2014  
 1159 computed by a manual identification of natural features visible in the shaded DEMs

1160 generated by **(a)** ALS for both survey epochs and by **(b)** ALS and photogrammetry  
1161 for 2003 and 2014 survey, respectively.